

Master Thesis Internship Report

Integration of a Tape Roll for Decay Spectroscopy to Control the Build-Up of Background Radioactivity

Khan, Muhammad Minhaj

Masters' Student – Nuclear Engineering

IMT Atlantique, France

Interdisciplinary Research Group
Institute For Nuclear and Radiation Physics
KU Leuven, Belgium

Supervisors:

Prof. Dr. Amanda Porta (IMT Atlantique)
Prof. Dr. Thomas Elias Cocolios (KU Leuven)



Table of Contents

1. Introduction.....	8
1.1 <i>Production of Exotic Isotopes at ISOLDE.....</i>	<i>10</i>
1.2 <i>Collinear Resonance Ionization Spectroscopy (CRIS).....</i>	<i>11</i>
2. Detection of Ions in DSS station for Decay Spectroscopy	13
2.1 <i>DSS – CF based Windmill System:</i>	<i>13</i>
2.2 <i>DSS2.0 – CF based Ladder System:</i>	<i>14</i>
2.3 <i>DSS+ Mylar® tape-based system:.....</i>	<i>15</i>
2.4 <i>Design Meeting – Integration</i>	<i>16</i>
3. Tape Station.....	20
3.1 <i>Old Tape Station:.....</i>	<i>20</i>
3.2 <i>New Tape Station:.....</i>	<i>21</i>
3.3 <i>Description of New Tape Box</i>	<i>21</i>
3.4 <i>Characterization:.....</i>	<i>24</i>
3.4.1 <i>Vacuum Vesting Test.....</i>	<i>24</i>
3.4.2 <i>Movement, Steps and Speed Testing of Tape Plate.....</i>	<i>25</i>
3.5 <i>Positioning of Tape Station at CRIS-CERN.....</i>	<i>27</i>
4. Decay spectroscopy of ^{120}Ag.....	29
4.1 <i>^{120}Ag Nuclear Structure and Decay Scheme:</i>	<i>29</i>
4.2 <i>GEANT4 Simulations.....</i>	<i>30</i>
5. Conclusion	35
5.1 <i>Future work - 2022 Beamtime</i>	<i>36</i>
6. Reference	38
7. Appendix.....	39
7.1 <i>Classes for GEANT4 code</i>	<i>39</i>

<i>Primary Generator Action</i>	39
<i>Detector Construction</i>	40
<i>Event Action</i>	44
<i>Stepping Action</i>	46
<i>Run Action</i>	47

List of Figures

Figure 1.1: CF based windmill system [1-2]	8
Figure 1.2: CF based ladder system [3]	9
Figure 1.3: CRIS setup at ISOLDE [Self-taken at CERN in July 2021]	10
Figure 1.4: Main steps prior to CRIS [5]	10
Figure 1.5: Simple flow chart for CRIS experiment [1-3, 6].....	11
Figure 1.6: Main step-by-step resonance ionization process at CRIS setup [10]	12
Figure 2.1: Detailed view of DSS CF based windmill system [1-2]	13
Figure 2.2: Detailed view of DSS2.0 implantation system.....	14
Figure 2.3: Mount # 1 for Annular PIPs and Collimator	15
Figure 2.4: Mount # 2 for Mount # 1 and Mount # 3.....	16
Figure 2.5: Mount # 3 for solid PIPs detector.....	16
Figure 2.6: Newly designed Tape Frame and Tape Wheel for DSS+	17
Figure 2.7: Simple version of Tape Frame. [as suggested by designer]	18
Figure 2.8: Full assembly of DSS+ tape-based implantation system	18
Figure 2.9: Full assembly of DSS+ implantation system. [Based on original design in Fig. 2.6 and Fig 2.7]	19
Figure 2.10: Re-designed tape frame [Based on original design in Fig. 2.6 and Fig 2.7]	19
Figure 3.1: Components of Old Tape Station	20
Figure 3.2: Front and Back view of old tape plate.....	21
Figure 3.3: Components of New Tape Station.....	21
Figure 3.4: TapeTransport Control (19M09) Software.....	22
Figure 3.5: TapeTransport Controller (19M09).....	22
Figure 3.6: Pictorial view of a stainless-steel Tape Box - (L x W x H) 825 x 400 x 628.4 mm	23

Figure 3.7: Front view of tape plate.....	23
Figure 3.8: Back view of tape plate	23
Figure 3.9: Vacuum Vesting test - old tape box with new machines	24
Figure 3.10: Movement Speed in relation to time with 1500 Steps.....	26
Figure 3.11: Steps in relation to time with 80 % speed	27
Figure 3.12: Positioning of CRIS DSS at CRIS - CERN	28
Figure 4.1: Partial decay of ^{120}Ag [15].	29
Figure 4.2: Beta Decay scheme of ^{120}Ag , ^{120}Cd , ^{120}In to stable ^{120}Sn	30
Figure 4.3: Classes of Geant4 implemented in in the simulation.	31
Figure 4.4: Geometry of ACOL, APIPS, Mylar® tape and PIPS detector constructed in GEANT4.....	32
Figure 4.5: Simulation for 1 beta decay (in red) and the resulting Gamma or X-ray (in green).	33
Figure 4.6: Simulation for 10 beta decays (in red) and the resulting Gamma or X-ray (in green)	33
Figure 4.7: Beta energy deposition spectrum on PIPs.	34
Figure 4.8: Beta energy deposition spectrum on APIPS.	34
Figure 5.1: Schedule for CRIS experiment in 2021.....	37
Figure 7.1: $1\text{E}10^7$ beta decay in the DSS+	48
Figure 7.2: Simulation for 1×10^7 beta events on Mylar® Tape	48
Figure 7.3: Simulation for 1×10^7 beta events on ACOL	48

Acknowledgement

I would like to extend my utmost gratitude to all those who encouraged me to bring this report to fruition. First, I would like to express my appreciation to my supervisor Prof. Dr. Thomas Elias Cocolios, for providing me the opportunity to work at the IOG group at the KU Leuven. I am deeply grateful for selecting me as his sub-ordinate (Intern), for his help at every step, professionalism, and valuable guidance throughout my entire period of internship. Also, I am thankful to him for putting his trust in me by sending me to ISOLDE – CERN for experiments twice for more than two weeks each. I must acknowledge, it has been a wonderful experience.

I would like to express my most profound appreciation to Dr. Hilde De Witte - Instrument Specialist at IKS, KU Leuven, for her mentorship during the period of my internship. I would like to thank her for teaching me about tape station, testing the tape station, and reviewing the work of my master report on the characterization of tape station.

My sincere appreciation to Silvia Bara for providing guidance on the tape station based on her knowledge and experience and overall support during my thesis internship. High five to Jake Johnson for answering my stupid questions related to nuclear physics and nuclear structure without getting annoyed! Thanks to Jake for organizing my birthday dinner with CERN experimental colleagues. I did not expect that!

My honest gratitude to various colleagues from York University, especially Dr. James Cubiss, for answering and solving physics questions for the GEANT4 simulation in the very last days when I needed help the most.

I want to thank Isabelle Boesmans for her help in all administrative matters. I appreciate her commitment to the work and dealing with our requests as well. Thank you so much for scheduling, remembering important dates and crucial administrative procedures without which we literally cannot move!

Finally, I am indebted to all the IOG group members for selecting me, teaching me, guiding me. I am thankful for your unfailing support and continuous encouragement throughout my internship. This accomplishment would not have been possible without your team's support.

With my sincere regards,

KHAN, Muhammad Minhaj

2021 – August – 25th

Abstract

This internship aims to minimize background radioactivity by devising a new design for the decay chamber of a decay spectroscopy station (DSS). The DSS is coupled to the collinear resonance ionization spectroscopy (CRIS) experiment at the end of its beamline at the Isotope Separator On Line DEvice (ISOLDE) facility at CERN in Switzerland. The CRIS experiment is dedicated to understanding the hyperfine structure of exotic nuclei, identifying exotic isotopes via their characteristic decays, and studying purified samples, including separated isomers.

The existing design of the DSS chamber, i.e., carbon foil-based ladder system, was replaced with Mylar® tape-based system by designing a new frame for the integration of Mylar® Tape for the DSS chamber. The new geometry was simulated with GEANT4 code to simulate beta decay of ^{120}Ag isotope and the detection of beta into the silicon detectors. The efficiency of two silicon detectors was found to be 81.93 % which is an excellent result obtained for simulating a ^{120}Ag beam implant on Mylar® tape as the distance from PIPS to Mylar® tape and APIPS to Mylar® tape is reduced in the new design.

In parallel, characterization studies for the existing and new tape station for IDS experiments were done at KU Leuven, and findings were used as a new reference point for the DSS for the CRIS experiment. The idea is to adopt the same design of the tape station being used for IDS and to make changes in the existing design of the DSS chamber where the beam will be implanted, including the experimental requirements of CRIS (e.g., ultra-high vacuum). As the CRIS experimental studies require ultra-high vacuum conditions, i.e., 10^{-10} mbar compared with IDS that requires only 10^{-6} mbar, vacuum conditions for the IDS' tape roll were tested twice: first with an empty chamber and then with tape plate integrated with tape roll, one stepper motor and two servo motors. As a result, the vacuum pump was operated for more than twenty-four hours, and the required vacuum pressure, i.e., 10^{-6} mbar, was achieved. However, this highlighted how a different solution must be investigated to reach the requirements for operation at CRIS.

Initial pre-experimental tests with the IDS tape station and the new tape frame design have been presented and discussed with the CRIS team at CERN during the CRIS Collaboration Meeting in the first week of May 2021. Recommendations from the CRIS collaboration were implemented in this study.

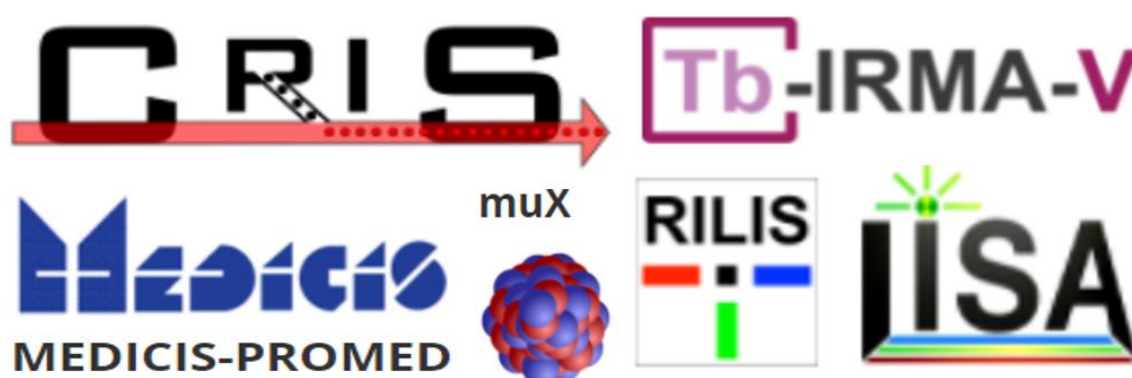
Keywords: Exotic isotopes, Nuclear Structure, ^{120}Ag , ^{120}Cd , Hyperfine structures, Resonance ionization, Laser spectroscopy, CRIS, ISOLDE, DSS, CERN

Interdisciplinary Research Group, KU Leuven

The research internship is carried out from 01st April 2021 to 30th September 2021 with the Interdisciplinary Research Group (IOG) at the KU Leuven Institute for Nuclear and Radiation Physics in the KU Leuven, Leuven, Belgium. KU Leuven is the #1 university in Europe for innovation. The IOG group is led by Prof. Dr. Thomas Elias Cocolios, a young and dynamic new professor at IKS, KU Leuven.

IOG group aims at bridging between the fundamental research of the Institute for Nuclear and Radiation Physics with more societal applications by having substantial involvement in both aspects but always centered around the use of exotic radioactive isotopes. From astrophysics to medicine, the IOG group covers a wide range of topics in Nuclear Structure, Nuclear Astrophysics, Medical Isotopes, and Societal Applications. In short, the IOG group covers from ground-state properties of very exotic nuclei to the production of medical isotopes and has substantial involvement with national and international partners as shown in below picture.

Currently, the IOG group has two postdocs, 5 Ph.D. students, and three master's students. IOG has plans to expand its research group and is currently in the process of acquiring funds for expanding its research on exotic isotopes.



IOG's involvement with national and international partners

Chapter 1

1. Introduction

The motivation of this work is to minimize the background radioactivity by devising a new design for the decay chamber of Decay Spectroscopy Station (DSS) coupled to the Collinear Resonance Ionization Spectroscopy (CRIS) experiment at the end of its beamline at Isotope Separator On Line DEvice (ISOLDE) facility at the CERN.

The previous design of DSS housed a carbon-foil (CF) based windmill system in the DSS chamber, as shown in Figure 1.1. However, the CF-based windmill system was replaced with the existing CF-based ladder system, called DSS2.0, due to the attenuation of gamma rays at low energies by the steel wall of the DSS chamber and the steel windmill Figure 1.2 shows the picture of the CF-based ladder system inside the decay chamber [1-3]. The proposed idea is to replace the CF-based ladder system with the Mylar® tape-based system due to the limited number of carbon foils (only 2~3), which become highly contaminated with the overpopulation of isobars and daughter nuclei of isotopes of interest [2-3].

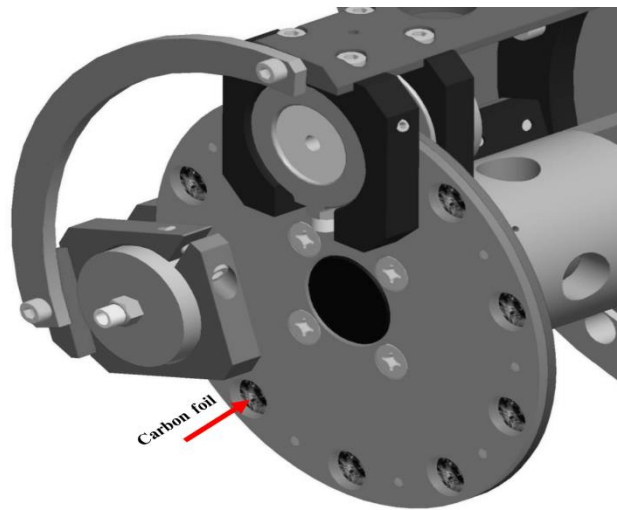


Figure 1.1: CF based windmill system [1-2]

The main goal is to avoid data acquisition from the decay of long-lived daughter nuclei, whose decays may contaminate the fresh acquisition of beam implantation. Furthermore, the Mylar® tape-based system is expected to be free from the limitations of overpopulation of daughter nuclides as it can easily be rolled for fresh implantation without opening the whole DSS chamber. In this study, the author feels excellent pleasure by working on the evolutionary

new design of DSS and would like to label Mylar® tape-based system as DSS+, which can be read as DSS plus.

As discussed above, DSS+ will be installed at the end of the CRIS beamline experiment to identify exotic isotopes via their characteristic decays and the study of purified samples, including separated isomers. A pictorial view of the CRIS setup at ISOLDE is shown in Figure 1.3, taken during the visit to CERN for the ISOLDE Decay Station experiment from 13th – 21st July 2021.

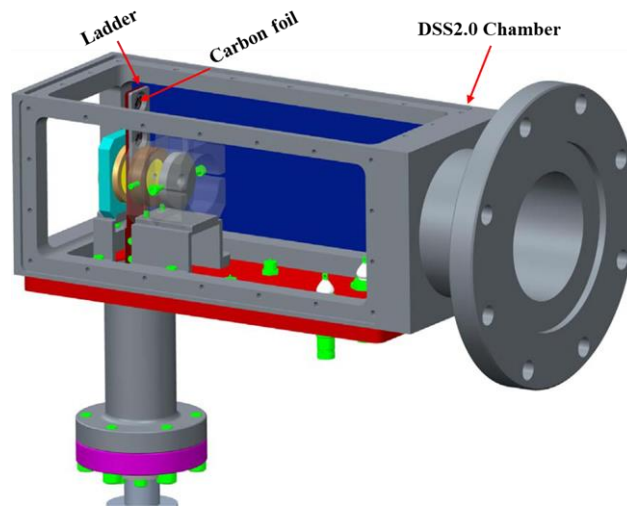


Figure 1.2: CF based ladder system [3]

The purpose of the CRIS experiment is to study the properties of exotic isotopes through the collinear resonance ionization spectroscopy technique. CRIS allows to further investigate the properties of rare isotopes and, in particular, their charge radius, its spin, and its nuclear electromagnetic moments. In conclusion, in one experiment, we can measure four observables of exotic isotopes, and we can compare those observables to the predictions of models. As this study mainly focused on studying and designing a new design for the CRIS DSS, few concepts from the production of exotic isotopes to their detection in DSS will be presented to showcase the evolution of learning during the period of this internship.

From the production of exotic isotopes to the detection of these isotopes into the DSS chamber, the whole experimental setup is mainly divided into three stages are tabulated below and will be discussed in sections 2, 3, and 4, respectively.

1. Production of exotic isotopes at ISOLDE

2. Collinear laser spectroscopy and resonance ionization spectroscopy – CRIS
3. Detection of ions into the DSS chamber for decay spectroscopy

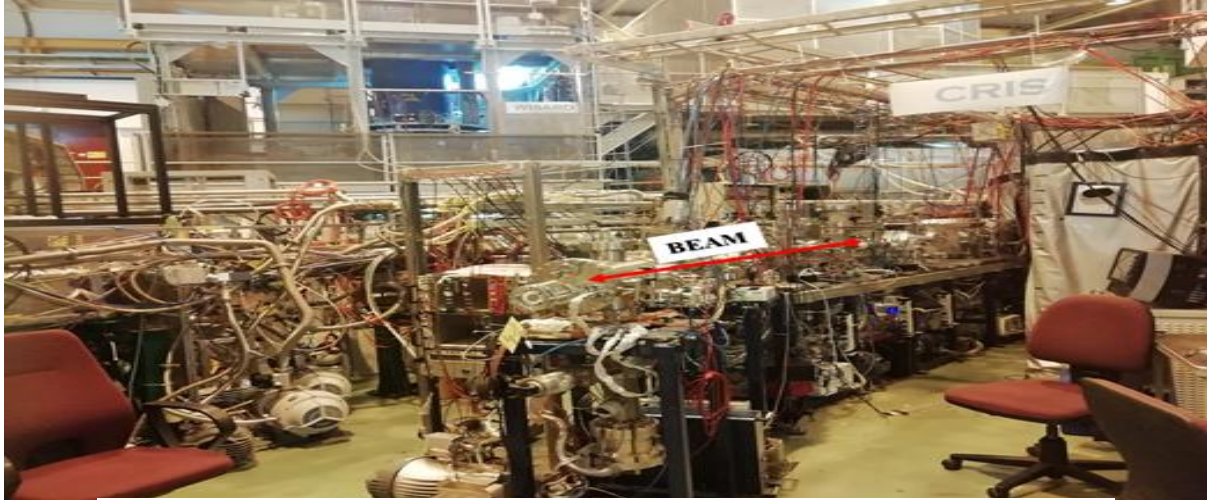


Figure 1.3: CRIS setup at ISOLDE [Self-taken at CERN in July 2021]

1.1 Production of Exotic Isotopes at ISOLDE

The ISOLDE facility employs CERN's accelerator complex for protons of energy equivalent to 1.4 GeV in order to produce exotic nuclei of most of the elements. These exotic in-nature radioactive nuclei are used for basic research in many areas of science: nuclear physics, nuclear astrophysics, atomic physics, condensed matter physics, radiobiology, and elementary particle physics. ISOLDE belongs to a network of radioactive beam facilities in Europe responsible for pure research and development of exotic nuclei. The ISOLDE facility generates beams of isotopes in a wide mass range (from $A = 6$ (Li) up to $A = 232$ (Ra), which are then delivered to several experiments being conducted at the ISOLDE for the purpose of fundamental and medical research [4]. Pictorial view of the ISOLDE experimental hall is

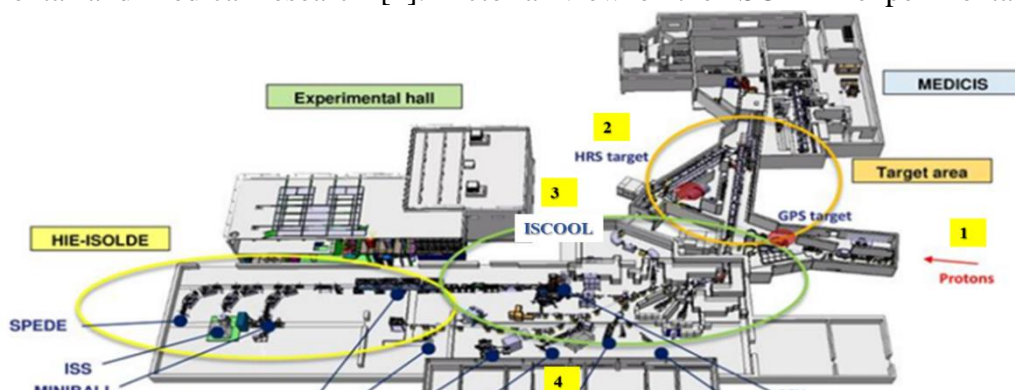


Figure 1.4: Main steps prior to CRIS [5]

shown in Figure 1.4, which shows the various experiments being conducted at ISOLDE and the main steps from the production of exotic isotopes to their delivery in bunched beam to CRIS setup [5].

The production of exotic isotopes begins by striking 1.4 GeV protons delivered by the Proton Synchrotron Booster on a thick target such as uranium carbide (UCx) or Thorium carbide (ThCx) [2,4]. These radioactive products are then surface ionized, accelerated to 30 keV, and mass separated with the high-resolution separator (HRS) to select the isotope of interest. The ions are then bunched using the radio-frequency quadrupole (RFQ) ISolde COOLer (ISCOOL). The cooling and bunching are done in order to provide the possibility of short bunches of a few microseconds in the length of bunched ions, which plays an important factor for an efficient CRIS experiment. [2, 6-8]. The bunched ions in short bunches of few microseconds in length are then delivered to the CRIS setup. A simple flow chart from the production to the delivery of radioactive beam to CRIS is shown in Figure 1.5 [1-3, 6].

1.2 Collinear Resonance Ionization Spectroscopy (CRIS)

This section serves to briefly explain the main components of the CRIS setup needed to run the CRIS experiment, through which decay spectroscopy of exotic isotopes is made possible. CRIS setup is divided into the neutralization of radioactive beams, the laser system, which resonantly ionizes bunched beams, and then the detection chamber i.e., DSS.

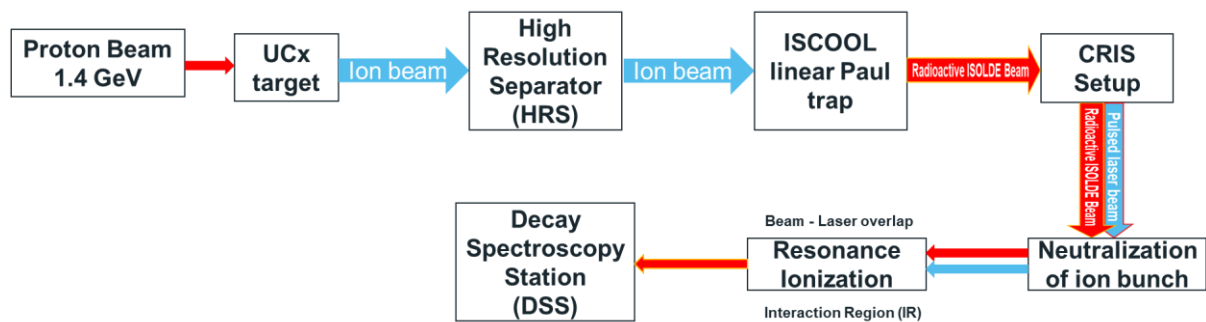


Figure 1.5: Simple flow chart for CRIS experiment [1-3, 6]

The bunched ions beam from ISCOOL neutralizes in a charge exchange cell (CEC) with alkali metal at the temperature of 150 °C with a background pressure of 10^{-6} mbar. This chamber is set after a 34° bend to overlap the ion and laser beams later [6, 9]. The neutral atom bunch is then guided through a differential pumping region while the non-neutralized component is deflected within the differential pumping region. The atom bunch is temporally

overlapped with the laser pulse in the interaction region, where the pressure is maintained under 10^{-8} mbar to minimize non-resonant collisional ionization [6, 9]. After passing the differential pumping region, the atom beam from CEC overlaps with the laser beams in the interaction region (IR), and that is when and where the real collinear resonance ionization occurs, as shown in Figure 1.5 and Figure 1.6. This region is kept at an ultra-high vacuum of 10^{-9} mbar to 10^{-10} mbar to suppress collisional excitations of the atoms. The atoms are then ionized in a two-step process through lasers. The first interaction of bunched beams happens with resonant laser that excites the atoms from the ground state to an excited state.

During the second interaction atoms in the excited state resonantly ionized by the lasers and then deflected into the DSS. A detailed description of the lasers utilized at the CRIS beamline can be found in Ref. [6, 9]. Figure 1.6 shows the main step-by-step resonance ionization process at CRIS setup [10], i.e., neutralization with alkali vapor, interaction with lasers, and deflection into the DSS.

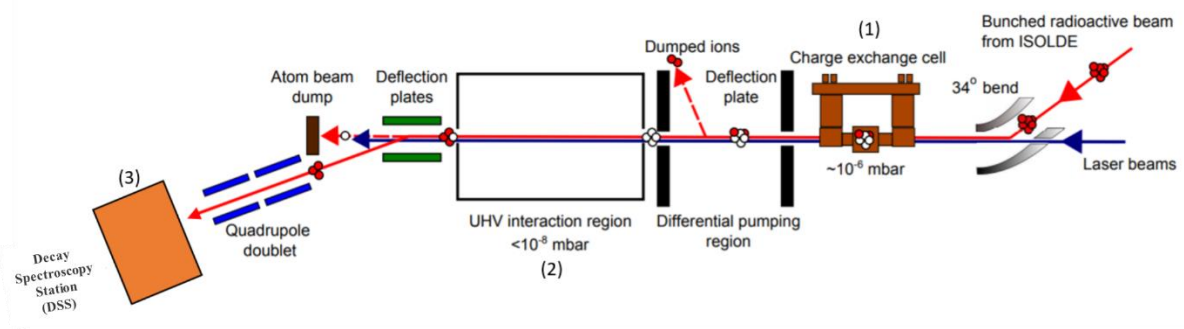


Figure 1.6: Main step-by-step resonance ionization process at CRIS setup [10]

Chapter 2

2. Detection of Ions in DSS station for Decay Spectroscopy

As stated in the introduction, the objective of this study is to devise a new design and positioning the DSS+ chamber. Previous designs of DSS have been briefly reviewed and discussed in comparison with the DSS+ design in this section. The final version of the DSS+ design is discussed in detail in Section 2.3.

2.1 DSS – CF based Windmill System:

The first version of the DSS designed in the 1990s consists of a rotating wheel implantation system, as shown in Figure 2.1 [1]. It is developed at KU Leuven and has provided results with several successful experiments [11 - 14]. The wheel holds ten thin carbon foils, with a thickness of 80 nm, where the beam of the ionized bunch is implanted. One Solid PIPs detector (Canberra Series A, 300 μm thick) places behind the carbon foil, and an annular PIPs detector (Canberra, Series AN, 300 μm thick) is placed exactly opposite to solid PIPs detector, for the purpose of detecting alpha decay. The ion beam is guided through the 4 mm hole of the

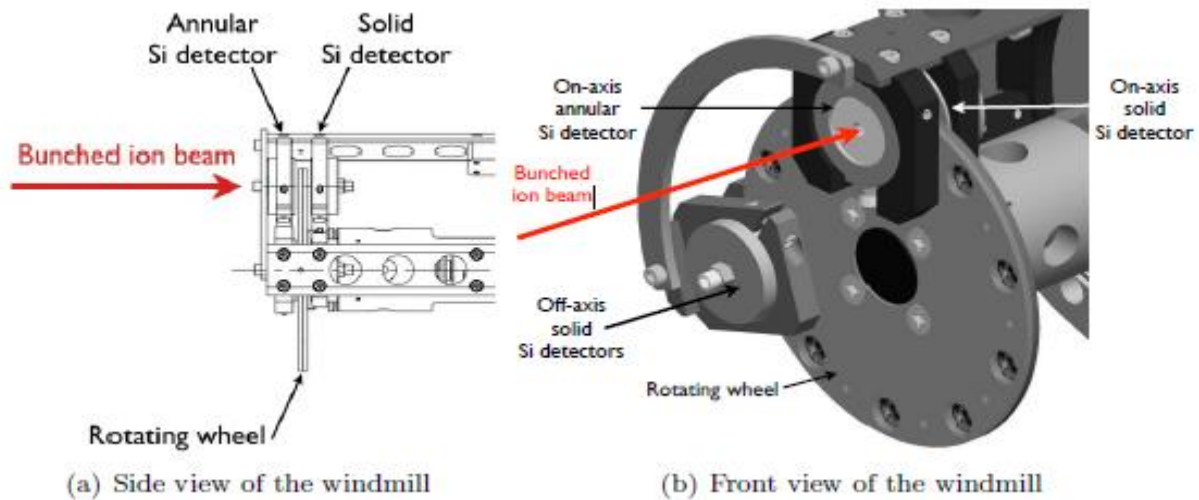


Figure 2.1: Detailed view of DSS CF based windmill system [1-2]

annular detector, which allows particle detection in response to backward recollision i.e., backward alpha / beta emission. In addition to the on-axis detectors, two solid PIPs silicon detectors are placed off-axis. This allows for measurements on longer-lived decay products to be performed by rotating the implanted foil from the on-axis to the off-axis detector position. [1-2].

2.2 DSS2.0 – CF based Ladder System:

The motivation for designing DSS2.0 is to minimize the attenuation and absorption of γ -ray by removing the windmill and the steel chamber. The windmill system, which holds carbon foils, and the steel chamber, which houses the windmill system, is replaced with the CF-based ladder system and the aluminium chamber.

Figure 1.2 shows the 3D representation of the DSS2.0 chamber. DSS2.0 chamber consists of a rectangular aluminium chamber (dimensions: $10 \times 10 \times 25$ cm) that can be mounted onto a DN100 vacuum flange. In order to minimize the γ -ray absorption, out of four, three side panels are braised, thin (2 mm) aluminium walls. The fourth panel is a base plate on which the sample holder, in-vacuum detectors, and associated connectors are placed. For alpha and beta

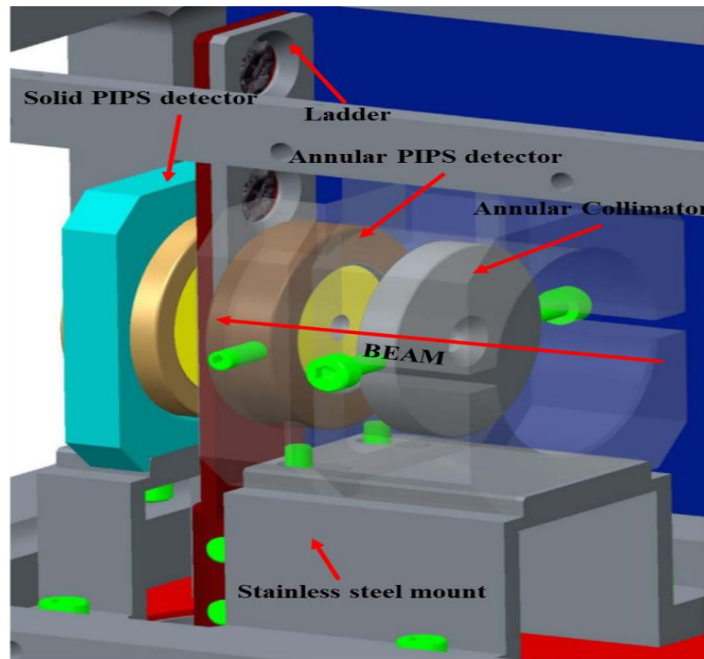


Figure 2.2: Detailed view of DSS2.0 implantation system.

spectroscopy, one solid and one annular passivated implanted planar silicon (PIPS) detectors are mounted on the stainless-steel mount, either side of an implantation site. A stainless-steel ladder holding two CFs and an insulated copper plate (used as a Faraday cup) is used as the implantation site. Figure 2.2 shows the detailed view of the implantation system of DSS2.0, i.e., PIPS and APIS detector, annular collimator, ladder, carbon foils, and beam implantation site. γ -ray detection efficiency is nearly a factor of 400 times better than the DSS. The performance of the DSS2.0 is found to be suitable for the planned future studies [3,6].

2.3 DSS+ Mylar® tape-based system:

The basic idea in designing a new beam implantation system is to remove the ladder and replace it with the Mylar® tape-based system to avoid excessive radioactivity by the overpopulation of daughter nuclides of the isotope of interest. The new and original design for the beam implantation site on DSS+, i.e., integration of tape system, mechanics, movement of the tape, is one of the main parts of this internship. The new design is idealized and drawn by utilizing Inventor® CAD software from AUTODESK.

The precondition of integrating Mylar® tape into the existing design of DSS2.0 is not making any design changes in the existing DSS2.0 chamber except in the mount for collimator and APIPs detector (Mount # 1) facing towards tape and Solid PIPS detector, the mount (Mount # 2) on which the Mount #1 stays and mount for solid PIPS detector (Mount # 3) facing towards tape and APIPs detector. Mount #1, Mount #2 and Mount #3 are shown in Figure 2.3, Figure 2.4, and Figure 2.5 respectively.

In order to integrate the Mylar® tape, a tape frame with the wheel attached to the shaft of the tape frame was designed. Figure 2.6 shows the design of the tape frame with the wheel.

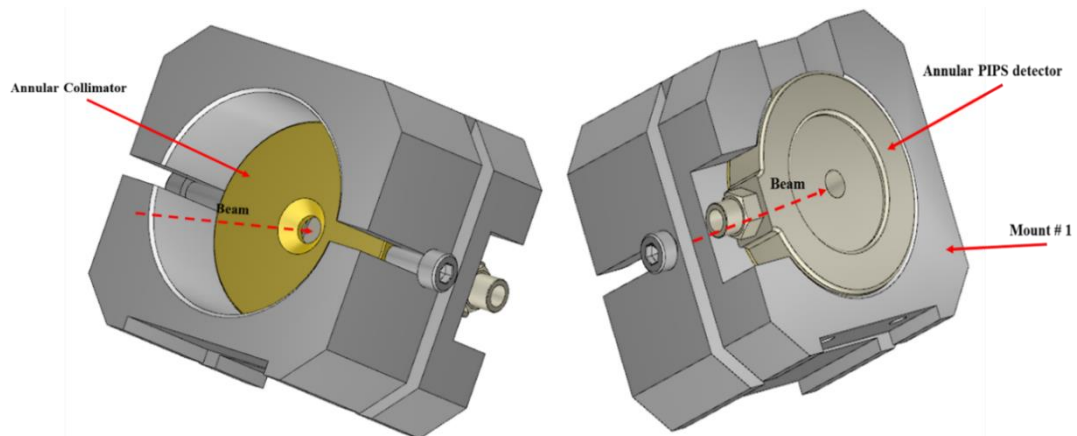


Figure 2.3: Mount # 1 for Annular PIPs and Collimator

The tape frame is the four-legged frame. Each leg is 71.929 mm in length and 4 mm in width. The width of the frame is 51.950 mm, and the length is 43.163 mm. The wheel shaft is 48 mm in length and 3mm in diameter is attached to the front-end of the frame, which helps to move the tape coming from and going into the tape station. The tape frame is screwed with four screws on either side of Mount #1, and the curved legs are attached with two screws on either side of Mount #2. The screws are 2.50 mm in diameter. This is done to keep the frame firm on

the mount during the tape's running on the wheel as the tape moves 60 cm in 250 milliseconds (ms). The details of the movement of tape are discussed in Chapter 3 for the characterization of tape station. Minor amendments in Mount #1 and Mount #2 were made in terms of dimensions and attachment of frame through screws. The complete assembly of a tape frame screwed and attached with mounts is shown in Figure 2.7.

2.4 Design Meeting – Integration

The original design drawn as part of the work during this internship presented in Figure 4.6

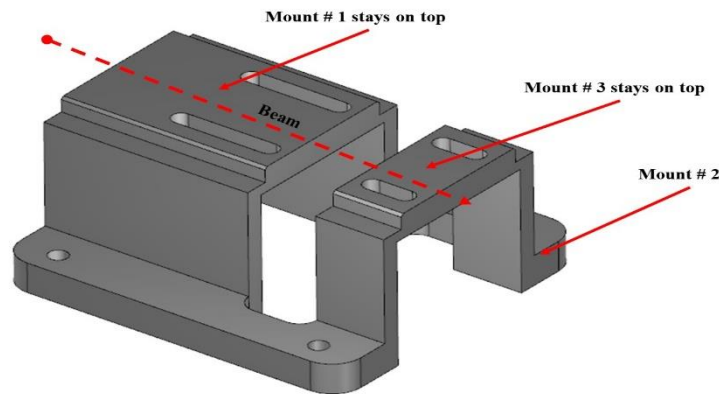


Figure 2.4: Mount # 2 for Mount # 1 and Mount # 3

and Figure 4.7 is then communicated to a professional design engineer at The University of Manchester in the first week of August following a design meeting on 9th August 2021. Based on the original design, the designer suggested a simpler version of the tape frame, as shown in Figure 4.7 (in pink colour). However, a simpler version of the design did not reflect the issues of vibration and tension on the tape frame and the stainless-steel mount.

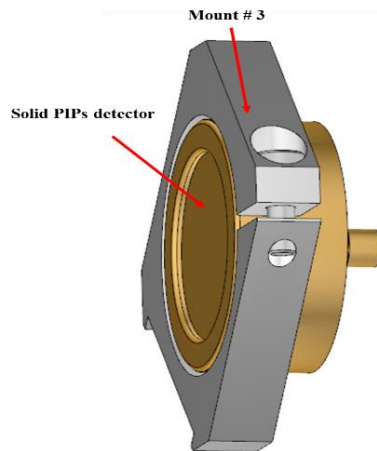


Figure 2.5: Mount # 3 for solid PIPs detector

On the basis of the original design made during this internship and from the perspective of manufacturing and production, manufacturing of Mount# 1 and tape frame in one single piece with a separate wheel system is suggested by the designer and agreed as a final design of the DSS + Mylar® tape-based system. The tape frame and the entire assembly is shown in Figure 4.9 and Figure 4.10 respectively.

As a consequence of removing the ladder, in both designs, the space between annular and solid PIPs detector has been reduced from 18 mm to 12 mm for better detection efficiency for the PIPs detectors. The reduction in space between the two PIPs detectors is meaningful as the tape does not require much space in terms of movement, and the nearer the tape is from the detectors, the better the detection efficiency for alpha and beta particles and for the spectroscopic studies.

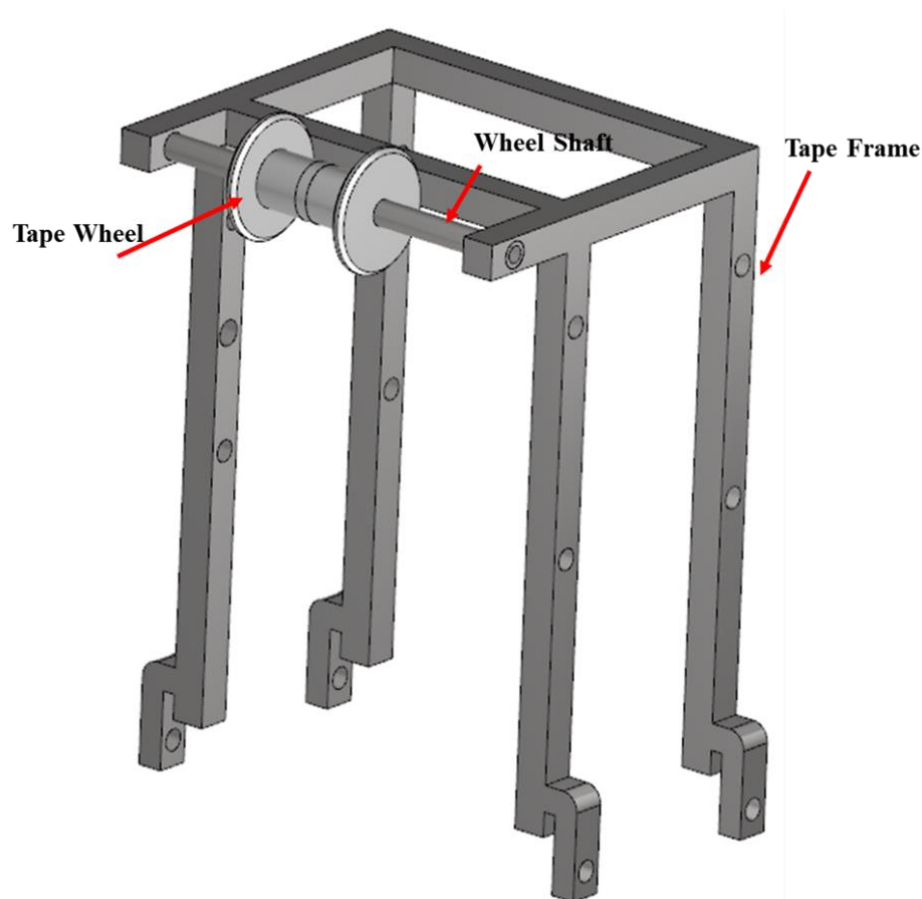


Figure 2.6: Newly designed Tape Frame and Tape Wheel for DSS+

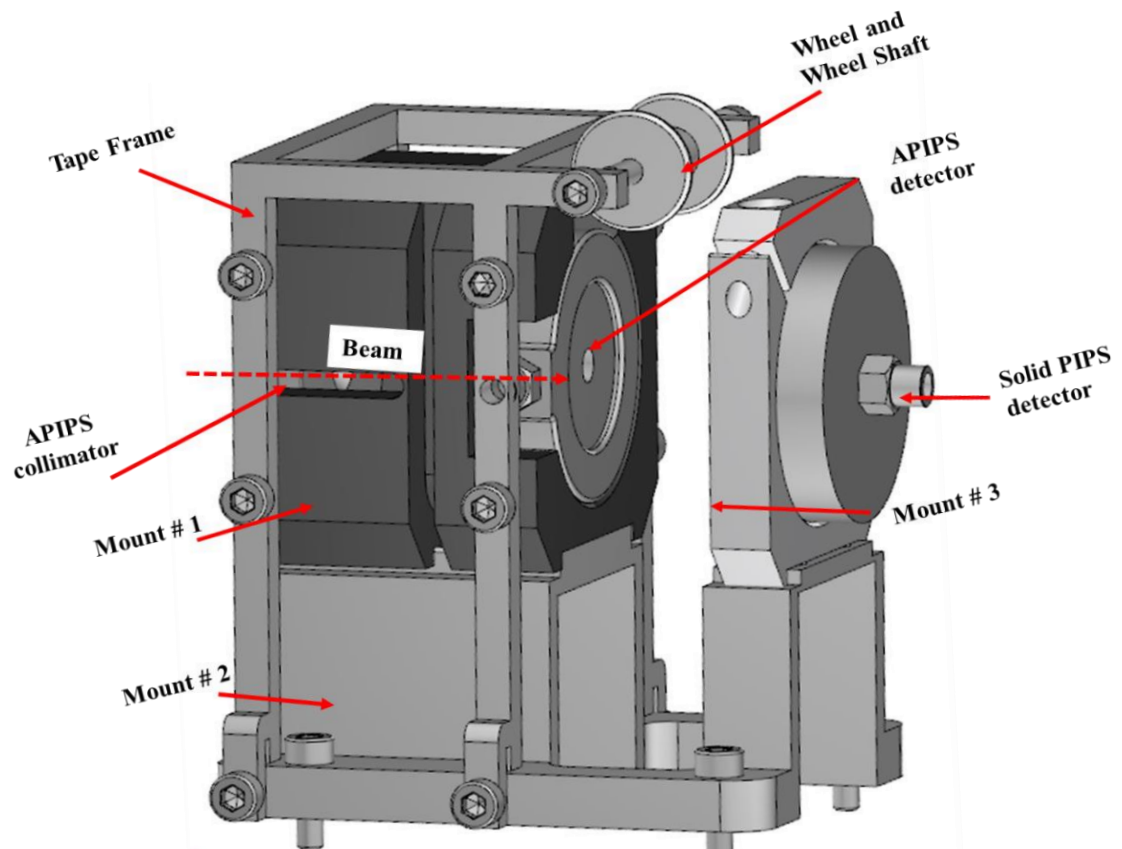


Figure 2.8: Full assembly of DSS+ tape-based implantation system

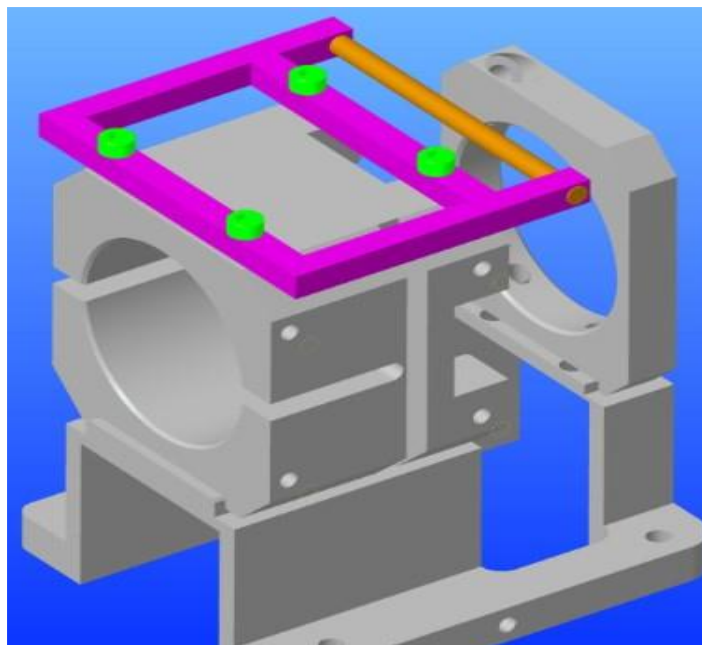


Figure 2.7: Simple version of Tape Frame. [as suggested by designer]

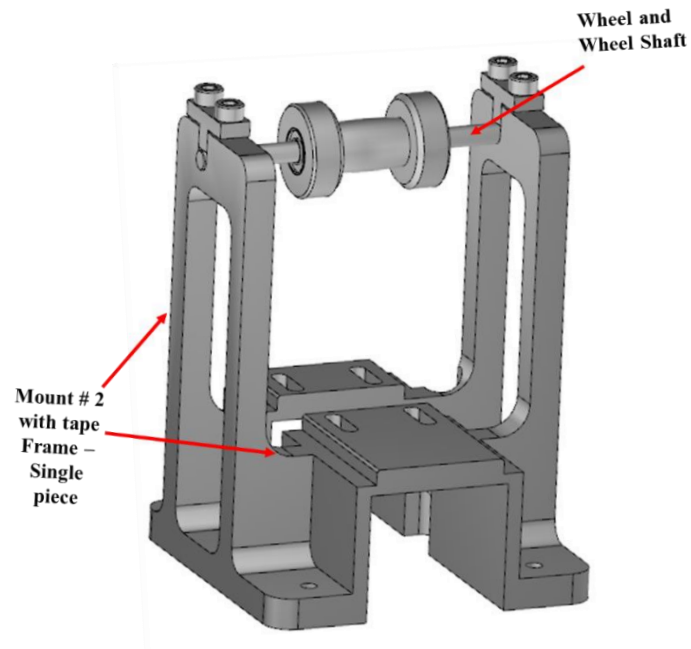


Figure 2.10: Re-designed tape frame [Based on original design in Fig. 2.6 and Fig 2.7]

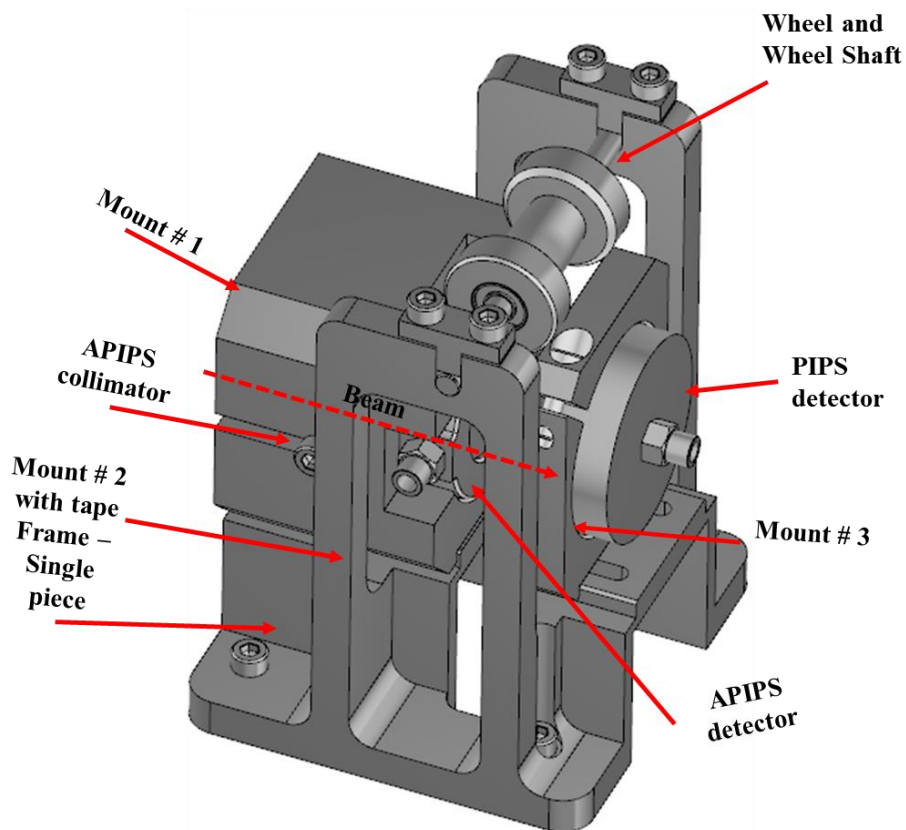


Figure 2.9: Full assembly of DSS+ implantation system. [Based on original design in Fig. 2.6 and Fig 2.7]

Chapter 3

3. Tape Station

As discussed in the previous chapter, the motivation in utilizing the Mylar® tape based acquisition system is to avoid data acquisition from the decay of long-lived daughter nuclei, where the decays of daughter nuclei may contaminate the fresh acquisition of beam implantation due to longer half-life than its mother. Therefore, the tape-based acquisition system is introduced to better understand the exotic isotopes with very short half-lives in the magnitude of hundreds of milliseconds (ms).

3.1 Old Tape Station:

The old tape station designed in the 1970s has been replaced with the newly designed tape station. Random faults such as leakage of oil from old servo motors, the precision of stepper motors which affects the movement of the tape, breaking and twisting of Mylar® tape due to the design of wheels and manual control for the movement of tape makes it difficult for the acquisition of data. For example, with the old tape system, the speed of the tape to move is

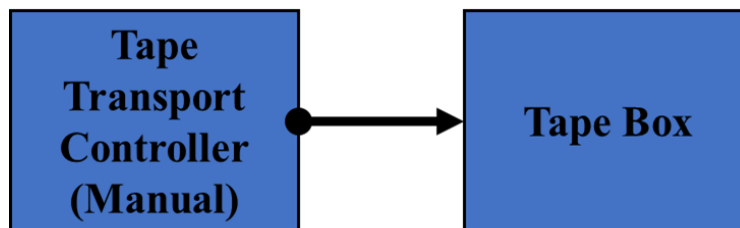


Figure 3.1: Components of Old Tape Station

800 ms per 60 centimetres (cm) of tape. As the half-lives of exotic isotopes are smaller compare with their daughters, increment in the speed of the tape to avoid build-up radioactivity from the overpopulation of daughter nuclides is complicated based on the existing design as it results in the twisting and breaking of tape. The old tape station consists of a Tape Box and manual Tape Transport Controller through which all the mechanical movements of tape can be controlled. The component-wise schematic of the old tape station is shown in Figure 3.1. Figure 3.2 shows the front side and backside of a tape plate for an old tape station.

3.2 New Tape Station:

The new tape station is an advanced version of an old tape station with improved controls, mechanics, and the swift movement of the tape. The new tape station consists of a Tape box, Tape Transport Controller, and software called “TapeStation Control (19M09)”

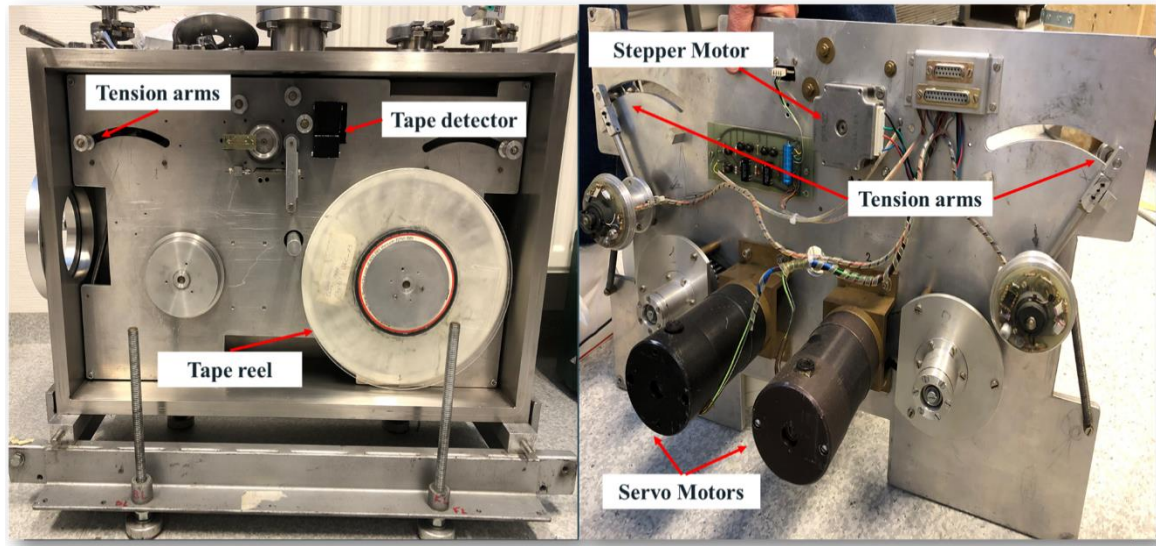


Figure 3.2: Front and Back view of old tape plate

developed at the KU Leuven installed in a laptop through which all the mechanical movements of tape can be controlled. Figure 3.3 shows the three components of the tape station. Figure 3.4, Figure 3.5, and Figure 3.6 show the pictures of TapeStation Control (19M09) software, TapeTransport controller (19M09), and Tape Box, respectively.

3.3 Description of New Tape Box



Figure 3.3: Components of New Tape Station

Figure 3.6 shows an actual picture of a tape box. A stainless-steel box with (L x W x H) 825 x 400 x 628.4 mm and weighs 187.73 kg when empty and approx. 200 kg, including the tape plate. The tape plate consists of one empty and one full tape reel, two servo motors connected to two tensor arms, which apply the force on tape to keep it stable, and a stepper

motor that precisely controls the movement of the tape. Figure 3.7 and Figure 3.8 show the front and backside of a tape plate, respectively. In the new design of the tape plate, the mechanical movement of tape is controlled through software to avoid human error and to increase the precision in the movement of the tape. Similarly, for the swift movement of the tape, wheels that help Mylar® tape to move are newly designed with high walls and bulge in the middle to keep the tape from slipping and twisting, as shown in Figure 3.7. Also, with the newly designed wheels, the speed of the tape to move is increased by 68.75 %, i.e., from 800 ms per 60 cm to 250 ms per 60 cm.

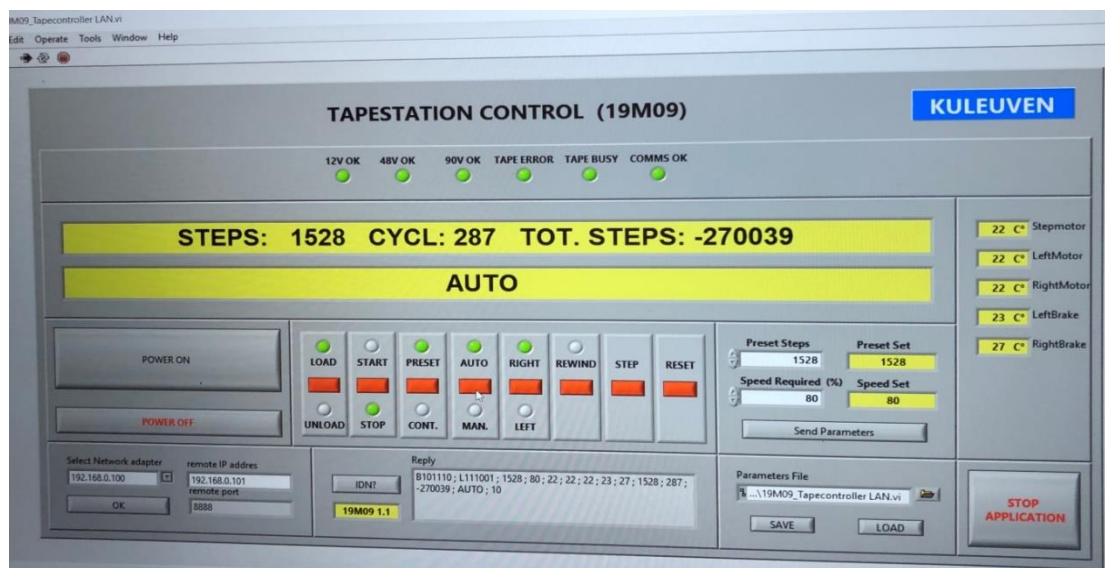


Figure 3.4: TapeTransport Control (19M09) Software



Figure 3.5: TapeTransport Controller (19M09)

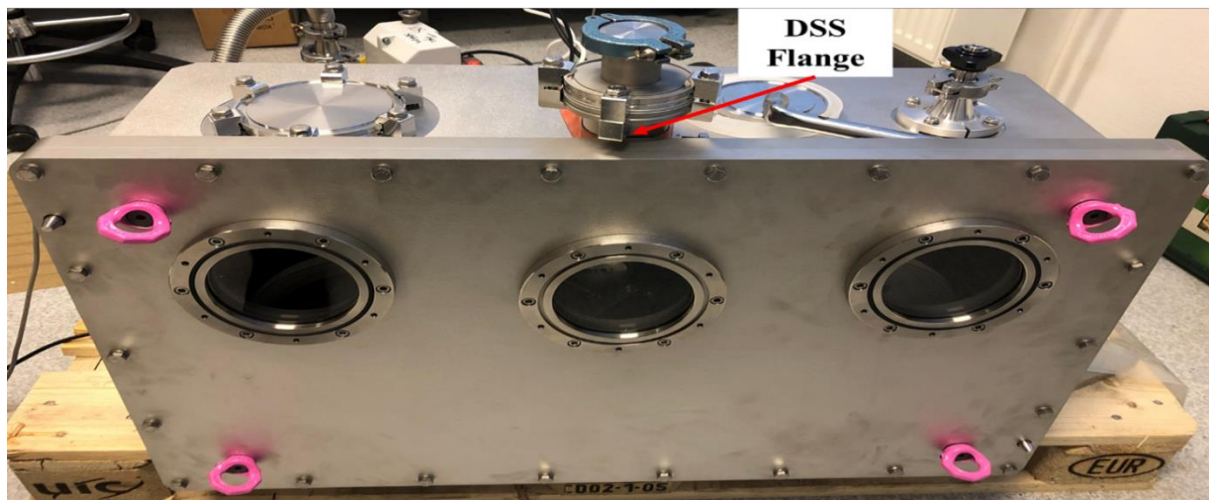


Figure 3.6: Pictorial view of a stainless-steel Tape Box - (L x W x H) 825 x 400 x 628.4 mm

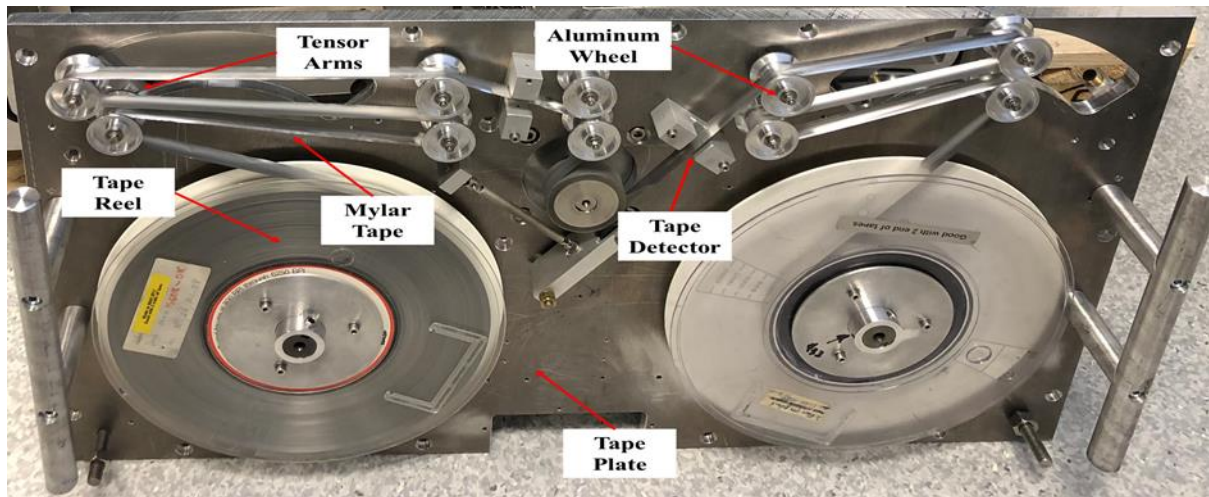


Figure 3.7: Front view of tape plate

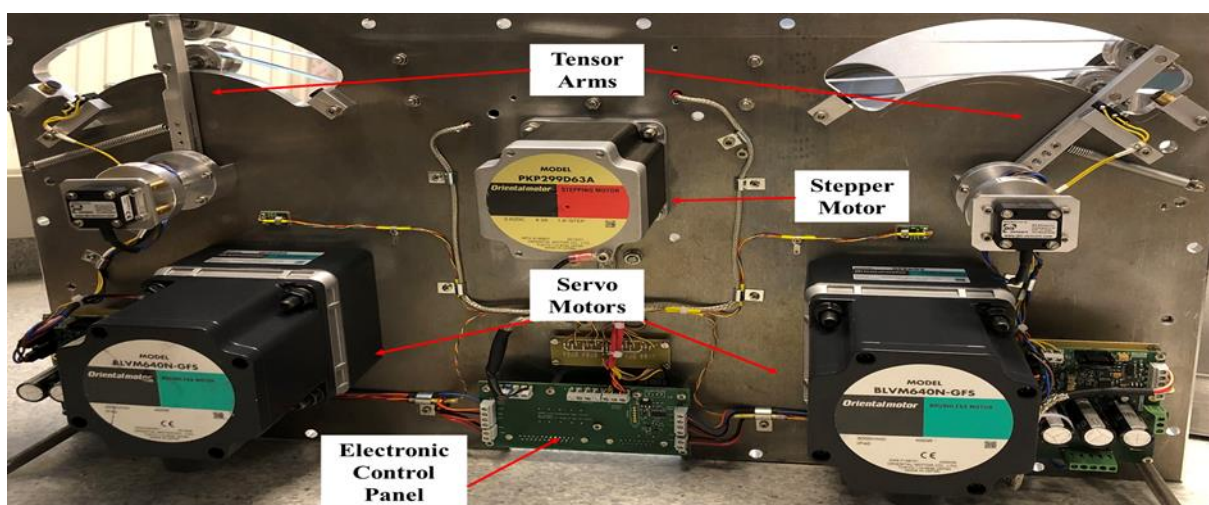


Figure 3.8: Back view of tape plate

3.4 Characterization:

New components of the new tape station have been tested for the first time. Unfortunately, the COVID19-crisis and the “Evergiven incident” in the Suez Canal caused the shortage of steel across Europe, resulting in the late manufacturing and delivery of new tape box by one and half months. As a result, the vacuum vesting test for the new tape box could not be done on time. However, new servo motors and electronic panels have been tested for vacuum vesting and discussed in detail in the section of the vacuum vesting. Similarly, the motion of tape, precision of stepper and servo motors were tested.

3.4.1 Vacuum Vesting Test

The CRIS experimental studies require ultra-high vacuum conditions, i.e., 10^{-10} mbar, compared with IDS that requires only 10^{-6} mbar. Vacuum conditions for the old IDS tape box with new servo motors and electronic panel were tested three times with Rotary Vane Pump in the beginning and then Turbopumps as the latter does not work under atmospheric pressure.

As shown in Figure 3.9, three vacuum vesting tests were run. The first test (shown in blue) is conducted with empty tape box. Vacuum pressure of 10^{-5} mbar was achieved in twenty-three hours due to several leaks and problems with the O-rings (seals) used in the tape box to make it vacuum-proof. During the second vacuum test (shown in orange), two servo motors and an electronic panel were put inside the tape box. As can be seen from Figure 3.9, the leakages

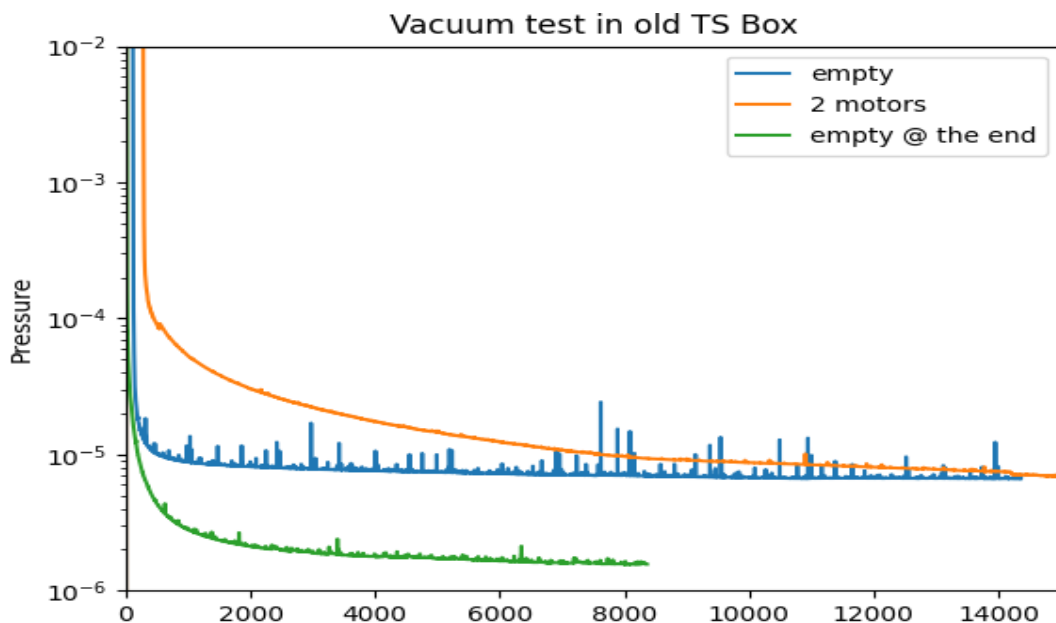


Figure 3.9: Vacuum Vesting test - old tape box with new machines

were reduced by 90 % due to the proper fitting of the tape box. However, the ideal vacuum condition of 10^{-5} mbar was not achieved after more than 23 hours of vesting. The vacuum test was repeated for the third time (as shown in green) with an empty tape box, and the required vacuum pressure, i.e., 10^{-6} mbar was achieved in less than 13.5 hours. For all three tests, the vacuum pump was operated for more than twenty-four hours. However, during the third run, as the ideal vacuum pressure was achieved in less than 24 hours, we stopped further vesting.

Please note that the time on the x-axis is in units of six bins and can be calculated by using Equation 1. For example, the time value of 2000 and 14000 is equivalent to 3.3 hours and 23,3 hours, respectively.

$$Time\ in\ hours\ (Hour) = \frac{Time\ Value\ (TV)}{3,600\ Seconds} \times 6\ seconds$$

3.4.2 Movement, Steps and Speed Testing of Tape Plate

The characterization of the new plate with stepper motor has been studied to check the tape's motion in relation to the stepper motor. Table 3.1 shows the comparison between steps and the displacement of tape. Each step of a stepper motor equivalent of 1.8 degree of rotation in stepper motor displaces the tape by 0.4 mm, and the displacement of tape was checked for 100, 200, 300, and 1500 steps. Interestingly, the tape displaced precisely 40, 80, 120, and 600 mm for 100, 200, 300, and 1500 steps which were randomly selected.

Table 3.1: Steps and displacement of tape

Steps	Displacement [mm]
100	40
200	80
300	120
1500	600

By keeping 1500 steps as a constant value, the movement speed of the stepper motor was studied in relation to time. Similarly, by keeping speed at 80%, steps of the stepper motors were analysed in relation to time. In terms of precision, we can see from Table 3.2 that at 80 % speed with 1500 steps, it takes 260 ms for the tape to move, and from Table 3.3, we can confirm the precision that at 1500 steps with 80% speed, it takes 262 ms for the tape to move. Thus, the movement of tape was accurate for 99.23 %, with an acceptable difference of 0.76 %. Graphical representation of Table 2 and Table 3 is shown in Figure 3.10 and Figure 3.11, respectively.

Please note that, the busy time was estimated with oscilloscope while the tape and motor is running and precision of the movement of tape cannot be estimated this way.

Table 3.2: Movement Speed in relation to time with 1500 Steps

Speed [%]	Time [ms]
10	1620
20	810
30	540
40	420
50	348
60	310
70	282
80	260
90	246
100	240

Table 3.3: Steps in relation to time with 80 % speed

Steps	Time [ms]
100	36
300	88
500	126
700	150
900	178
1100	209
1300	234
1500	262
2000	334
2500	400

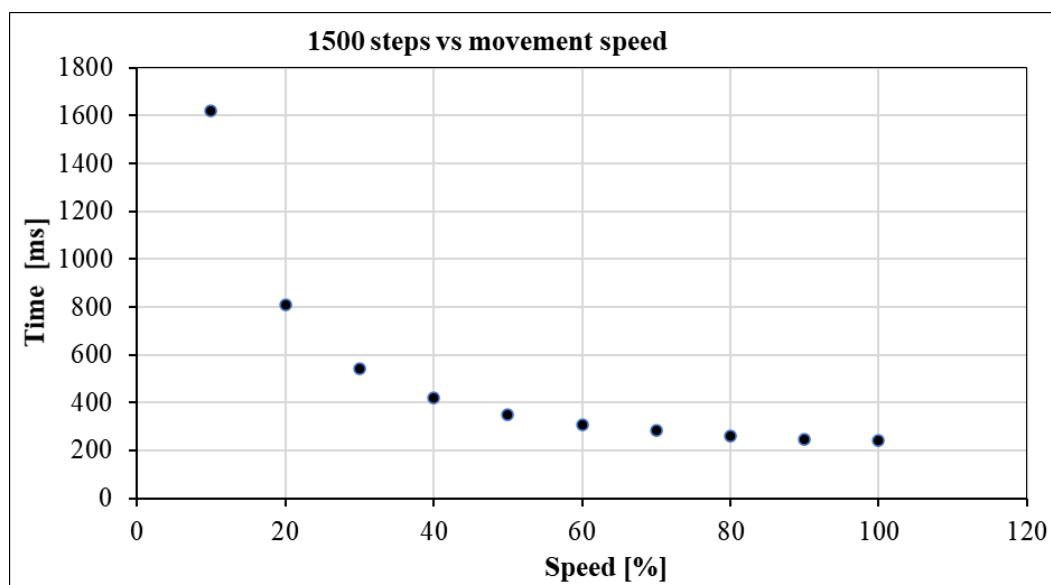


Figure 3.10: Movement Speed in relation to time with 1500 Steps

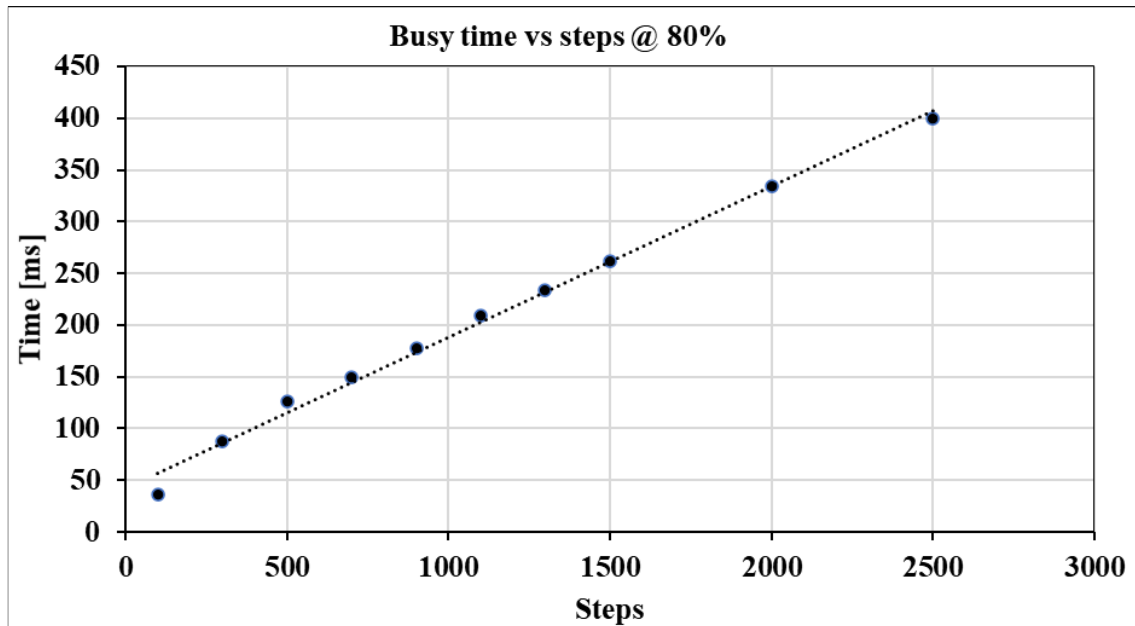


Figure 3.11: Steps in relation to time with 80 % speed

3.5 Positioning of Tape Station at CRIS-CERN

Upon visiting ISOLDE - CERN for two weeks in July 2021 to observe and participate in the IDS experiment, the positioning of CRIS DSS has been visualized. Figure 3.12 shows the possible positioning of CRIS DSS, which includes a DSS chamber attached to a tape station on a stainless steel trolley. As can be seen from Figure 3.12, besides the limited space, DSS can be easily fit along with its components, i.e., DSS chamber, new tape station, stainless steel trolley to move the whole setup. This study also proposes building a frame for the three germanium detectors that surround the DSS chamber to detect gamma activity during an experiment.

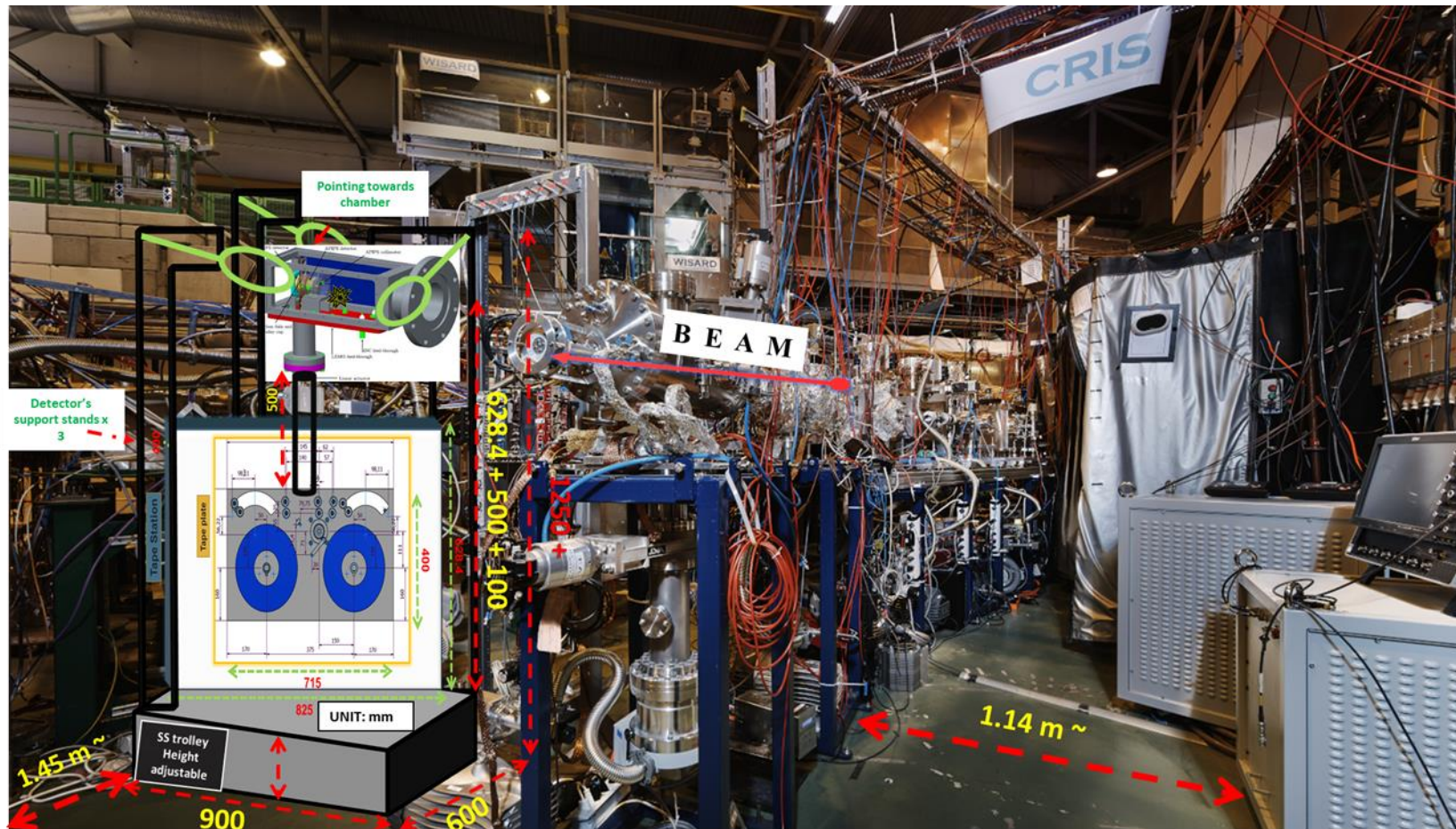


Figure 3.12: Positioning of CRIS DSS at CRIS - CERN

Chapter 4

4. Decay spectroscopy of ^{120}Ag

Decay spectroscopy is used to determine the decay properties of radioactive nuclei, by observing the particles emitted from the nucleus when it changes species. The motivation of this work is to study the nuclear structure of ^{120}Ag which is an exotic isotope from neutron rich region and has 47 protons and 73 neutrons. It features a ground state and two long-lived isomers, all of which may be studied at the CRIS experiment. Thanks to the high-resolution laser ionization, those isomers may be produced in isolation of each other, making their study at the CRIS DSS very attractive.

One the pure beam of ^{120}Ag ions is resonantly ionized by several pulsed laser, ions go into DSS+ chamber to be implanted on the Mylar® Tape, where beta decay is observed through silicon detectors (APIPS and PIPS).

4.1 ^{120}Ag Nuclear Structure and Decay Scheme:

Figure shows the partial decays of ^{120}Ag into two isomeric states through gamma decay and to the ground state via beta decay at 203.2 KeV. When ^{120}Ag is at the isomeric state at m3 7(-) there are two cases. First there is a high probability (approx. 68%) of going into the isomeric state of m2 4(+) where the half-life of ^{120}Ag is 1.52 s and then it can go into the second isomeric state at m1 (0-,1-) where the half-life is approx. 0.94 s. On the other hand, there is still a 32% probability for ^{120}Ag to go into ground state through beta decay and convert into ^{120}Cd . The x and y at m1 and m2 isomeric states shows the energies of low-spin isomers which can

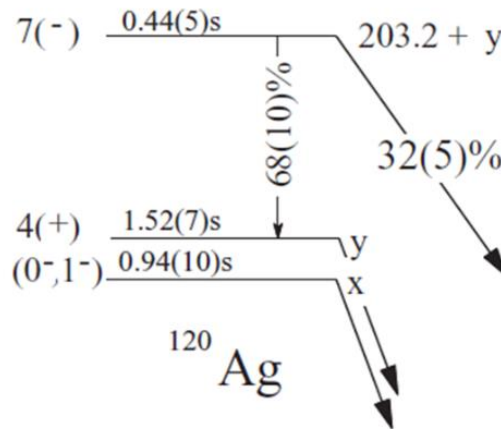


Figure 4.1: Partial decay of ^{120}Ag [15].

not be calculated through this work. ^{120}Ag will decay into ^{120}Cd through beta minus decay which is a primary decay product of ^{120}Ag .

Figure 4.2 shows the primary decay products through the beta decay of ^{120}Ag into ^{120}Cd . As can be seen from the Figure 4.2 that the half-life of ^{120}Cd is 50.8s which is 97.57 % more than the half-life of ^{120}Ag . ^{120}Cd then beta decays into ^{120}In (indium) whose half-life is 3.08 s, which is almost 60 % higher than the half-life of ^{120}Ag . ^{120}In then beta decays into ^{120}Sn which is a stable isotope.

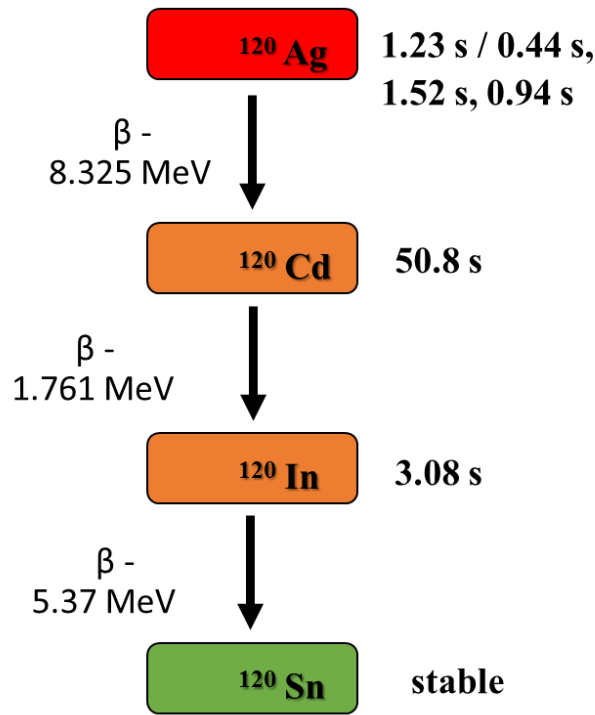


Figure 4.2: Beta Decay scheme of ^{120}Ag , ^{120}Cd , ^{120}In to stable ^{120}Sn

The difference in half-life of primary decay products of ^{120}Ag forms the basis of CRIS experiment. CRIS is dedicated to the study of the nuclear structure of ^{120}Ag , which is exotic in nature due to 1.23 s, 0.44 s, 1.52 s and 0.94 s of half-life at the ground state, m3 isomeric state, m2 isomeric state and m1 isomeric state respectively. As the experiment is concentrated on studying the ^{120}Ag but due to the longer half-life of ^{120}Cd , the study gets interrupted due to the over population of ^{120}Cd and ^{120}In and diminishing of ^{120}Ag .

4.2 GEANT4 Simulations

Monte Carlo simulations in physics are particularly important, as they help to foresee the results before an experiment. Geant4 is an object-oriented Monte Carlo simulation code, written in the C++ language, which has a hierarchical, modular and very flexible structure. The

implementation of the physical models is open and transparent. The code can handle interactions of particles with matter across a wide energy range [16].

Decay of ^{120}Ag has been investigated utilizing Geant4 code, simulated inside the decay chamber of DSS+ on aluminized Mylar® Tape, PIPS and APIPS detector, and annular collimator. The code is divided into different classes such as geometry, physics, particles etc. which all have their own working groups to keep improving the code.

Geant4 (**version geant4.10.6**) is used in this work to reproduce the decay of ^{120}Ag isotopes on Mylar® Tape and to detect beta energy deposition spectrum in PIPS, APIPS detector mainly. The different classes used to construct this simulation are schematically shown in Figure 4.3. It should be noted that the Physics list, Primary Generator and Detector Construction classes are constructed by the candidate. Crucial support and guidance were taken in making Stepping action and Event Action classes to simulate the beam of ^{120}Ag from various colleagues from The University of York in UK, who visited CERN for the ^{178}Au experiment at CERN from 18th August 2021 to 3rd September 2021. All the relevant Geant4 classes coded and used for this simulation written are defined in Appendix section at the end of the report.

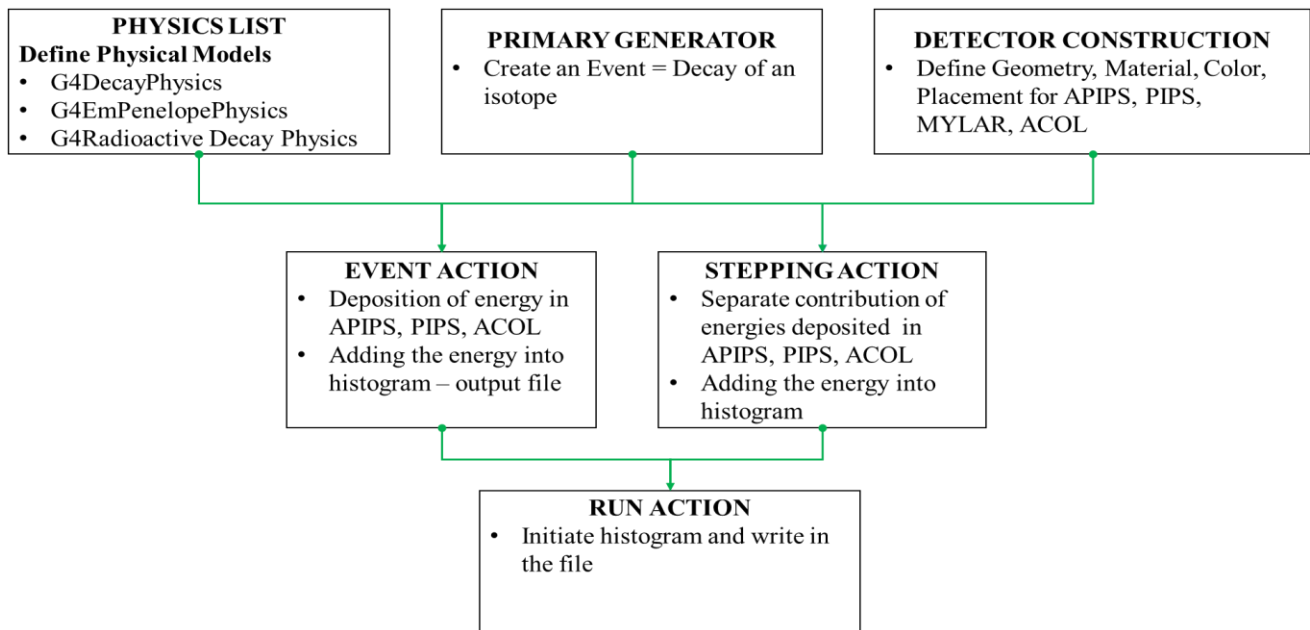


Figure 4.3: Classes of Geant4 implemented in in the simulation.

The geometry of APIPS, PIPS, ACOL and Mylar® tape is defined in the detector construction class is shown in Figure 4.4. In this study, ^{120}Ag beam was simulated, and beta particle was deposited on the surface of Mylar® tape to simulate the energy deposition in result of beta decays into PIPS and APIS detector mainly. Figure 4.5 shows the scattering of one beta particle

(in red) with Mylar® tape and the resulting gammas or x-rays (in green). Initially the simulation was run for 1 beta decay and then simulation was repeated for 10 and 10^7 beta decay events. Figure 4.6 shows the simulation of geometry with 10 beta decays.

Figure 7.1 in appendix shows the simulation of 10^7 beta events. Figure 4.6, Figure 4.7 shows the beta spectrum of energy deposition in PIPS and APIPS detector respectively. Figure 7.2 and Figure 7.3 in appendix shows the beta spectrum of energy deposition in Mylar® tape and ACOL.

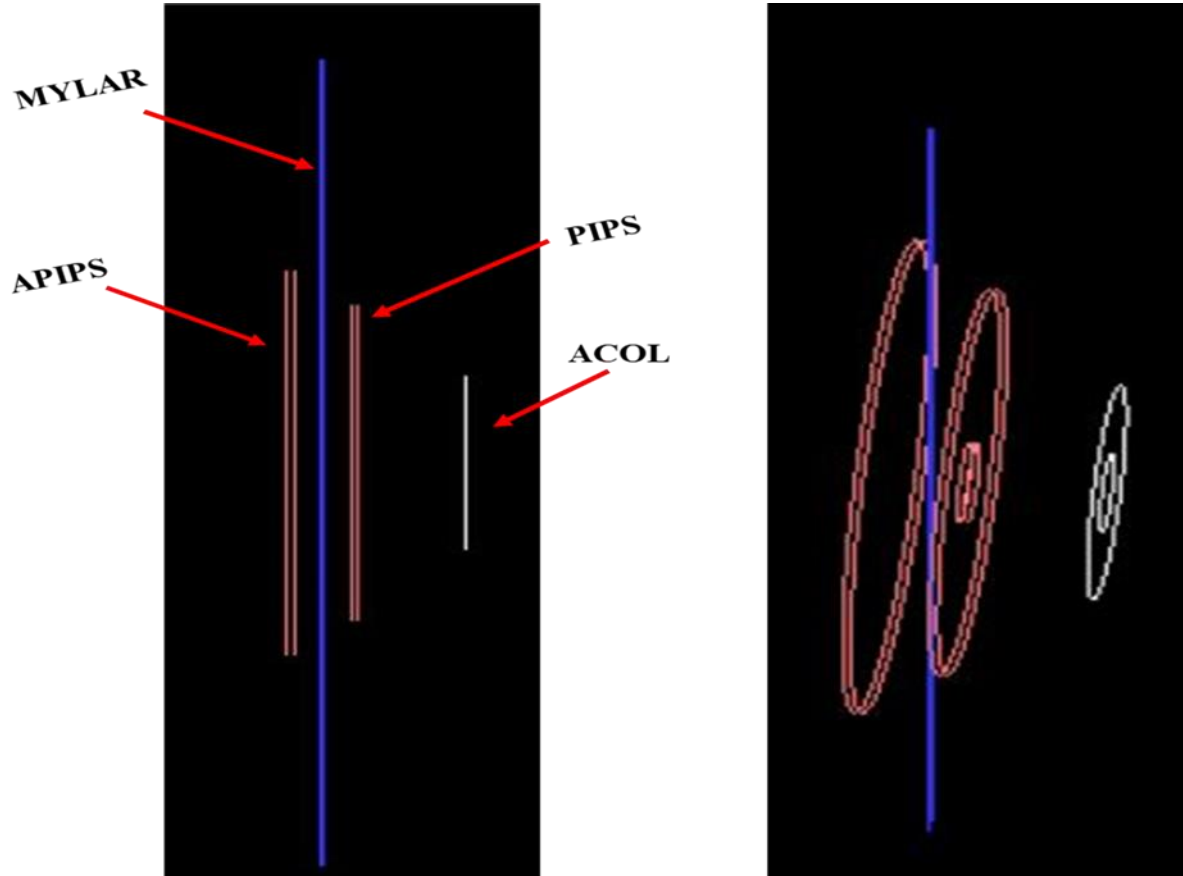


Figure 4.4: Geometry of ACOL, APIPS, Mylar® tape and PIPS detector constructed in GEANT4.

The purpose of this is to visualize the beta decay spectrum and to simulate the energy deposition especially for beta decays.

As can be seen in Figure 4.7 for PIPS detector, out of 10^7 beta events, 50,793,71 events were detected which shows the detection efficiency of 50.7 % of PIPS detector with the maximum counts of 140×10^3 at 0.25 MeV and less than 10×10^3 counts at 3 MeV. In case of APIPs in Figure 4.8, detection efficiency is 31.23 % with the detection of 3,123,983 beta events with approx. 50,000 counts at 0.45 MeV and less than 1,000 counts at 3.5 MeV. For Mylar®, beta source on the surface of the Mylar® tape was placed and detects 110^7 beta events 0.42 MeV is

the maximum energy deposited with $2,000 \times 10^3$ counts at energy 0.03 MeV. It is remarkable that the energy spectrum stops at 3 MeV while the beta particles have up to 8 MeV. This means

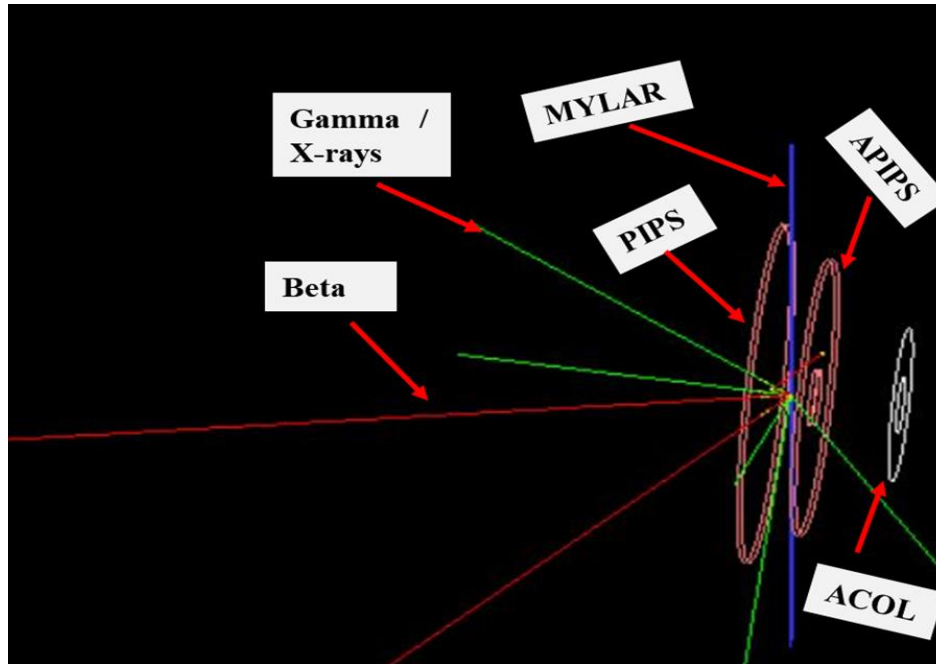


Figure 4.5: Simulation for 1 beta decay (in red) and the resulting Gamma or X-ray (in green). that the high-energetic particles only deposit part of their energy in the active volume of the detector. While the measured energy is proportional to the particle energy, this spectrum is better used as a trigger, or to perform some discrimination between low-energy and high-energy particles. Moreover, the simulation does not consider that the detector has a low-energy threshold below which the signal is not recorded; this should result in a slightly lower efficiency when measured experimentally.

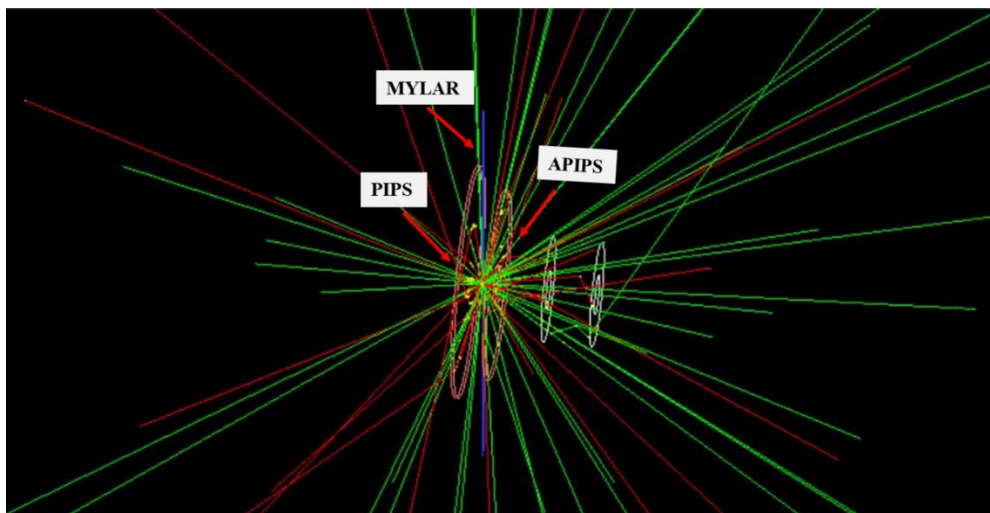


Figure 4.6: Simulation for 10 beta decays (in red) and the resulting Gamma or X-ray (in green)

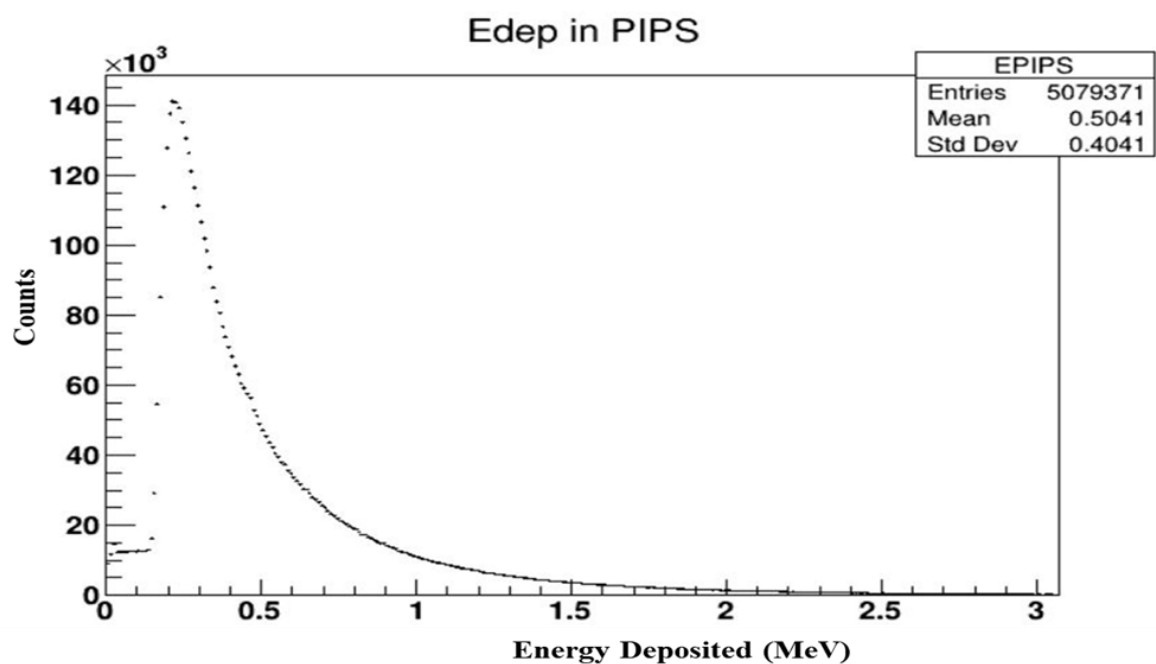


Figure 4.7: Beta energy deposition spectrum on PIPs.

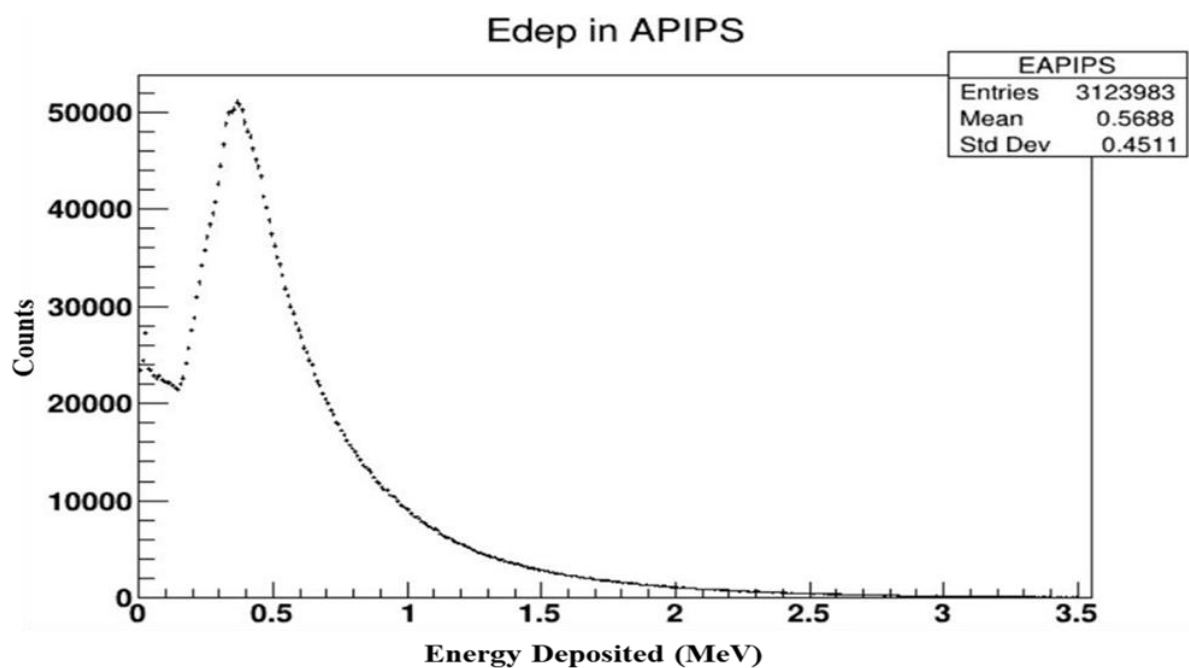


Figure 4.8: Beta energy deposition spectrum on APIPs.

Chapter 5

5. Conclusion

The first task of this internship is to do a literature search and study for the various designs and developments for the CRIS DSS experiment. Therefore, various publications and thesis produced by the IOG group, CRIS collaborators were studied and listed in the references.

The second task of the internship is to present and discuss the findings from the mechanical characterization of old tape stations being used for the IDS experiment during the CRIS collaboration meeting. The existing faults and the new findings of the old tape station, and the findings for the mitigation of existing IDS stations faults were presented and discussed during the CRIS collaboration meeting on May 5th, 2021. It was an excellent opportunity to represent the IOG group from KU Leuven during the CRIS meeting under the supervision of my tutor Prof. Dr. Thomas Elias Cocolios and collect feedback from experts belonging to CERN and various European research institutes.

The third task of this internship is to study the IDS tape station, analyze and assess from the perspective of materialization for the CRIS experiment. A step-by-step analysis of the whole tape station is presented. Due to the requirement of the CRIS experiment and the shortcomings of the old tape station, solutions presented here will be adopted for the CRIS experiment. For example, the vacuum vesting test highlighted how a different solution must be investigated to reach the requirements for operation at CRIS as an ideal vacuum for the CRIS experiment which is 10^{-10} mbar. This task was done under the supervision of technical staff, and experiments were done together.

The fourth task of this internship is to devise an idea to minimize the radioactivity by replacing the CF-based ladder system with Mylar® tape-based system from the DSS chamber for decay spectroscopy for the CRIS experiment. The frame for integrating Mylar® tape DSS+ chamber for CRIS experiment was built by utilizing AUTODESK Inventor software. It was an extraordinary experience to draw something directly for the CERN's experiment, which will be used for other experiments at ISOLDE.

The fifth task of this internship is to simulate the new design for DSS+ chamber with Geant4 and FLUKA code for the alpha/beta particles. In this study, simulations were done by using

Geant4 code to simulate the decay of ^{120}Ag . Due to time constraints, only Geant4 simulations were successfully done with Mylar® Tape, PIPS APIPS, and ACOL. PIPS and APIPS detector's efficiency were found to be 50.7 % and 31.2 %, which are a substantial improvement with respect to DSS2.0 (65% total efficiency). The physics list, detector construction, primary generator, and run action classes were constructed by me. I took help from a couple of Geant4 experts in making event action and stepping action classes.

The sixth task of this internship is to attend, observe and conduct the relevant experiment by visiting CERN. I have visited ISOLDE – CERN twice in July, from 12th to July 21st, 2021, for the IDS Thallium experiment. I visualized the working of the tape station, volunteered for the night shift experiment. At the end of the experiment, I assisted local staff in calibrating the germanium detector utilizing CAEN COMPAS software. My second visit to CERN is from August 18th to September 4th, 2021, for the ASET experiment. I helped my team in assembling and setting up our experimental setup at CERN. The actual beam time is starting from August 26th, 2021, and I am looking forward to participating in the experiment.

5.1 Future work - 2022 Beamtime

This internship was perfectly aligned with the expected CRIS experiment in June 2021 and September 2021 for ^{120}Ag as proposed by IKS, KU Leuven. Two experiments were scheduled, as shown in Figure 5.1, and one was conducted in June 2021. However, during June 2021, results were not received as expected, and a new target was needed for the second experiment, but it was not possible by September 2021. As a result, the upcoming experiment in September was canceled, and now the new beamtime is planned next year.

As the beamtime for the CRIS experiment has been postponed till 2022, the manufacturing of the new design of DSS+ tape roll would be possible until an actual experiment time. Indeed, it would be an excellent opportunity to visualize the manufactured tape-frame and be a part of an experiment in which the significant contribution was made during this internship in terms of re-designing the implantation chamber to be able to verify the minimization of background radioactivity caused by the over-population of daughter nuclides of ^{120}Ag mainly ^{120}Cd and to explore the nuclear structure of exotic isotopes in detail.

HRS schedule 2021													
	June				July				August				
WK	23	24	25	26	27	28	29	30	31	32	33	34	35
MO	7	14	21	28	5	12	IS622 19	#717 UC 26	2	9	16	23	30
TU					IS666	#653 UC n	IS666	IS680 30Mg	IS666				
WE		#715 UC	IS660		IS666 (sharing with GPS)	IS622	IS666 (nights)	@ >7.5MeV/u					
TH			CRIS		IS666	IS622	IS666	IS680 30Mg		#XXX LaC	IS661	(tbc) #715	IS660
FR					IS666	IS622	IS666	IS680 30Mg					
SA					IS666	IS622	IS666	IS680 30Mg					
SU					IS666	IS622	IS666	IS680 30Mg					
			RILIS: Ag		26Na	RILIS: Cu	26Na	RILIS: Mg	RILIS: Mg		RILIS: In		RILIS: Ag



Start of protons for physics: 21 June
End of protons for physics 15 November

Target change	CERN holiday	Setting up/proton scan/yield	Physics HPS	Physics GPS	RILIS run
---------------	--------------	------------------------------	-------------	-------------	-----------

Figure 5.1: Schedule for CRIS experiment in 2021.

6. Reference

1. Lynch, K.M, et al. "Laser assisted decay spectroscopy at the CRIS beam." Rutherford Centennial Conference on Nuclear Physics. IOP Publishing, 2012. 381.
2. Lynch, K.M, et al. "Laser assisted decay spectroscopy at the CRIS beam." *Hyperfine Interact* (2013): 95-101.
3. Lynch, K.M, et al. "A simple decay-spectroscopy station at CRIS-ISOLDE." *Nuclear Instruments and Methods in Physics Research Section A: Accelerators, Spectrometers, Detectors and Associated Equipment*. (2016): 14-18.
4. Rondelez, N, "Collinear Resonance Ionisation Spectroscopy of Neutron Deficient Tin." Master Thesis. KU Leuven, 2020.
5. Richard, C, "Off-line physics at ISOLDE during LS2." Presentation during 10th LS2 committee meeting. 31st March 2017.
6. Cocolios, T.E, et al, "The Collinear Resonance Ionization Spectroscopy (CRIS) experimental setup at CERN-ISOLDE." *Nuclear Instruments and Methods in Physics Research Section B: Beam Interactions with Materials and Atoms* (2013): 565-569.
7. Richter B, et al. "More than three decades of ISOLDE physics." *Hyperfine Interactions* (2000): 1-22.
8. Mané, E, et al. "An ion cooler-buncher for high-sensitivity collinear laser." *THE EUROPEAN PHYSICAL JOURNAL A* (2009): 503 - 507.
9. Procter, T.J, et al. "Development of the CRIS (Collinear Resonant Ionisation Spectroscopy) beam line." *Journal of Physics: Conference Series*, 2012.
10. I. Budinčević, et al. "Laser spectroscopy of francium isotopes at the borders of the region of reflection asymmetry." *PHYSICAL REVIEW* (2014): 014317.
11. Dendooven, P, 1992 Ph.D. Thesis Katholieke Universiteit Leuven
12. Cocolios, T.E, "Single-Particle and Collective Properties around Closed Shells probed by In-Source Laser Spectroscopy." PhD Thesis. KU Leuven, 2010.
13. A. N. Andreyev et al. "New Type of Asymmetric Fission in Proton-Rich Nuclei." *PHYSICAL REVIEW LETTERS* (2010): 252502.
14. Cocolios, T.E, et al, "Structure of ^{191}Pb from α - and β -decay spectroscopy." *JOURNAL OF PHYSICS G: NUCLEAR AND PARTICLE PHYSICS* (2010).
15. Batchelder, J.C, et al. "Low-lying collective states in ^{120}Cd populated by β decay of ^{120}Ag : Breakdown of the anharmonic vibrator model at the three-phonon level." *PHYSICAL REVIEW C* (2012): 064311.
16. S. Agostinelli, et al. "Geant4—a simulation toolkit." *Nuclear Instruments and Methods in Physics Research* (2003): 250 - 303.

7. Appendix

7.1 Classes for GEANT4 code

Primary Generator Action

```
/// \file B4PrimaryGeneratorAction.cc
/// \brief Implementation of the B4PrimaryGeneratorAction class

#include "B4PrimaryGeneratorAction.hh"

#include "G4RunManager.hh"
#include "G4LogicalVolumeStore.hh"
#include "G4LogicalVolume.hh"
#include "G4Box.hh"
#include "G4Event.hh"
#include "G4ParticleGun.hh"
#include "G4ParticleTable.hh"
#include "G4ParticleDefinition.hh"
#include "G4SystemOfUnits.hh"
#include "Randomize.hh"

#include "G4GeneralParticleSource.hh"
#include "G4Event.hh"

#include <math.h>

//.....ooo00000ooo.....ooo00000ooo.....ooo00000ooo.....ooo00000ooo.
//.....

B4PrimaryGeneratorAction::B4PrimaryGeneratorAction()
: G4VUserPrimaryGeneratorAction(),
  fParticleGun(nullptr)
{
  fParticleGun = new G4GeneralParticleSource();
}

//.....ooo00000ooo.....ooo00000ooo.....ooo00000ooo.....ooo00000ooo.
//.....

B4PrimaryGeneratorAction::~~B4PrimaryGeneratorAction()
{
  delete fParticleGun;
}

//.....ooo00000ooo.....ooo00000ooo.....ooo00000ooo.....ooo00000ooo.
//.....

void B4PrimaryGeneratorAction::GeneratePrimaries(G4Event* anEvent)
{
  // Set gun position
  //fParticleGun->SetParticlePosition(G4ThreeVector(0., 0., -
worldZHalfLength));
  fParticleGun->SetParticlePosition(G4ThreeVector(0., 0., 0.));
  fParticleGun->GeneratePrimaryVertex(anEvent);
}

//.....ooo00000ooo.....ooo00000ooo.....ooo00000ooo.....ooo00000ooo.
//.....
```

Detector Construction

```
#include "B4DetectorConstruction.hh"
#include "G4Material.hh"
#include "G4Tubs.hh"
#include "G4LogicalVolume.hh"
#include "G4PVPlacement.hh"
#include "G4SystemOfUnits.hh"
#include "G4NistManager.hh"
#include "G4Box.hh"
#include "G4Polycone.hh"
#include "G4Polyhedra.hh"
#include "G4RotationMatrix.hh"
#include "G4Transform3D.hh"
#include "G4SystemOfUnits.hh"
#include "G4PhysicalConstants.hh"
#include "G4SDManager.hh"
#include "G4MultiFunctionalDetector.hh"
#include "G4PSEnergyDeposit.hh"
#include "G4SubtractionSolid.hh"
#include "G4Colour.hh"
#include "G4VisAttributes.hh"
#include "G4RunManager.hh"
#include "G4GenericMessenger.hh"
#include "G4AutoDelete.hh"
#include "G4GlobalMagFieldMessenger.hh"
#include "G4VisAttributes.hh"
#include "G4Colour.hh"

//.....ooo00000ooo.....ooo00000ooo.....ooo00000ooo.....ooo00000ooo.
.....

G4ThreadLocal
G4GlobalMagFieldMessenger* B4DetectorConstruction::fMagFieldMessenger =
nullptr;

B4DetectorConstruction::B4DetectorConstruction()
:G4VUserDetectorConstruction()
{
    DefineMaterials();
}

//.....ooo00000ooo.....ooo00000ooo.....ooo00000ooo.....ooo00000ooo.
.....

B4DetectorConstruction::~B4DetectorConstruction()
{
}

//.....ooo00000ooo.....ooo00000ooo.....ooo00000ooo.....ooo00000ooo.
.....

//
//DEFINE MATERIALS
//

void B4DetectorConstruction::DefineMaterials()
{
    G4double a, z;
    G4double density;
```



```

G4int ncomponents, natoms;

G4NistManager* man = G4NistManager::Instance();

man->FindOrBuildMaterial("G4_Si");
man->FindOrBuildMaterial("G4_MYLAR");

new G4Material("Galactic", z=1., a=1.01*g/mole, density=
universe_mean_density,
                kStateGas, 2.73*kelvin, 3.e-18*pascal);
}

//
//DEFINE OBJECTS
//
G4VPhysicalVolume* B4DetectorConstruction::Construct()
{

//Check overlap of volumes
G4bool checkOverlaps = true;

// Define dimensions
// APIPS
G4double innerRadiusAPIPS = 4*mm;
G4double outerRadiusAPIPS = 19.5 *mm;
G4double hzAPIPS = 0.3*mm;
G4double startAngleAPIPS = 0.*deg;
G4double spanningAngleAPIPS = 360*deg;

// PIPS
G4double innerRadiusPIPS = 0*mm;
G4double outerRadiusPIPS = 23.9*mm;
G4double hzPIPS = 0.3*mm;
G4double startAnglePIPS = 0*deg;
G4double spanningAnglePIPS = 360*deg;

// Collimator
G4double innerRadiusACOL = 4.*mm;
G4double outerRadiusACOL = 10.8*mm;
G4double hzACOL = 5.00*mm;
G4double startAngleACOL = 0*deg;
G4double spanningAngleACOL = 360*deg;

// Mylar
G4double MYLAR_hx = 1.12*mm;
G4double MYLAR_hy = 100*mm;
G4double MYLAR_hz = 0.12*mm;


//BOX
//MINWORLD //MINWORLD=world
G4double MINWORLD_hx = 200*mm;
G4double MINWORLD_hy = 200*mm;
G4double MINWORLD_hz = 200*mm;

// Get materials
G4Material* defaultMaterial = G4Material::GetMaterial("Galactic");
G4Material* detectorMaterial = G4Material::GetMaterial("G4_Si");
G4Material* tapeMaterial = G4Material::GetMaterial("G4_MYLAR");

```

```

// Place volumes
G4Box* MINWORLDBox = new G4Box("World", MINWORLD_hx/2, MINWORLD_hy/2,
MINWORLD_hz/2);

G4LogicalVolume* worldLV =
    new G4LogicalVolume(MINWORLDBox,    //its solid
        defaultMaterial,    //its material
        "World");    //its name

G4VPhysicalVolume* worldPV =
    new G4PVPlacement(0,    //no rotation
        G4ThreeVector(),    //at (0,0,0)
        worldLV,    //its logical volume
        "World",    //its name
        0,    //its mother volume
        false,    //no boolean operation
        0,
        checkOverlaps);    //copy number

//APIPS

G4Tubs* APIPSTube
    = new G4Tubs("APIPS",
        innerRadiusAPIPS,
        outerRadiusAPIPS,
        hzAPIPS,
        startAngleAPIPS,
        spanningAngleAPIPS);

//logicalvolume
G4LogicalVolume* logicAPIPS =
    new G4LogicalVolume(APIPSTube,    //its solid
        detectorMaterial,    //its material
        "APIPS");    //its name
//placemnet

fAPIPSPV =
    new G4PVPlacement(0,    //no rotation
        G4ThreeVector(0, 0, 3*mm),    //at (0,0,0)
        logicAPIPS,    //its logical volume
        "APIPS",    //its name
        worldLV,    //its mother volume
        false,    //no boolean operation
        0,
        fCheckOverlaps);    //copy number

//dimensions - PIPS

G4Tubs* PIPSTube
    = new G4Tubs("PIPS",
        innerRadiusPIPS,
        outerRadiusPIPS,
        hzPIPS,
        startAnglePIPS,
        spanningAnglePIPS);

//logicalvolume

```

```

G4LogicalVolume* logicPIPS =
    new G4LogicalVolume(PIPSTube,    //its solid
        detectorMaterial,    //its material
        "PIPS");    //its name
//placemnet

fPIPSPV =
    new G4PVPlacement(0,            //no rotation
        G4ThreeVector(0,0,-3*mm), //at (0,0,0)
        logicPIPS,                //its logical volume
        "PIPS",                  //its name
        worldLV,                  //its mother volume
        false,                    //no boolean operation
        0,                        //copy number
        fCheckOverlaps);

//dimensions - ACOL

G4Tubs* ACOLTube
    = new G4Tubs("ACOL",
        innerRadiusACOL,
        outerRadiusACOL,
        hzACOL,
        startAngleACOL,
        spanningAngleACOL);

//logicalvolume

G4LogicalVolume* logicACOL =
    new G4LogicalVolume(ACOLTube,    //its solid
        detectorMaterial,    //its material
        "ACOL");    //its name
//placemnet

fACOLPV =
    new G4PVPlacement(0,            //no rotation
        G4ThreeVector(0,0, 18.5*mm), //at (0,0,0)
        logicACOL,                //its logical volume
        "ACOL",                  //its name
        worldLV,                  //its mother volume
        false,                    //no boolean operation
        0,                        //copy number
        fCheckOverlaps);

//Construct the Mylar-foil

G4Box* MYLARBox
    = new G4Box("MYLAR", MYLAR_hx/2, MYLAR_hy/2, MYLAR_hz/2);

G4LogicalVolume* logicMYLAR =
    new G4LogicalVolume(MYLARBox,    //its solid
        tapeMaterial,    //its material
        "MYLAR");    //its name

//placemnet

fMYLARPV =

```

```

        new G4PVPlacement(0,          //no rotation
                          G4ThreeVector(0,0,0), //at (0,0,0)
                          logicMYLAR,      //its logical volume
                          "MYLAR",         //its name
                          worldLV,         //its mother volume
                          false,            //no boolean operation
                          0,
                          checkOverlaps); //copy number

//
// Visualization attributes
//
worldLV->SetVisAttributes (G4VisAttributes::GetInvisible());

auto detectorAtt= new G4VisAttributes(G4Colour(1.0,0.5,0.5));
auto collimatorVisAtt= new G4VisAttributes(G4Colour(1.0,1.0,1.0));
auto simpleBoxVisAtt= new G4VisAttributes(G4Colour(0.2,0.2,1.0));

simpleBoxVisAtt->SetVisibility(true);
logicMYLAR->SetVisAttributes(simpleBoxVisAtt);
logicPIPS->SetVisAttributes(detectorAtt);
logicAPIPS->SetVisAttributes(detectorAtt);
logicACOL->SetVisAttributes(collimatorVisAtt);

    return worldPV;
}

void B4DetectorConstruction::ConstructSDandField()
{
    // Create global magnetic field messenger.
    // Uniform magnetic field is then created automatically if
    // the field value is not zero.
    G4ThreeVector fieldValue;
    fMagFieldMessenger = new G4GlobalMagFieldMessenger(fieldValue);
    fMagFieldMessenger->SetVerboseLevel(1);

    // Register the field messenger for deleting
    G4AutoDelete::Register(fMagFieldMessenger);
}

```

Event Action

```

/// \file B4aEventAction.cc
/// \brief Implementation of the B4aEventAction class

#include "B4aEventAction.hh"
#include "B4RunAction.hh"
#include "B4Analysis.hh"

#include "G4RunManager.hh"
#include "G4Event.hh"
#include "G4UnitsTable.hh"

#include "Randomize.hh"
#include <iomanip>

//.....ooo00000ooo.....ooo00000ooo.....ooo00000ooo.....ooo00000ooo.
//.....

B4aEventAction::B4aEventAction()

```

```

: G4UserEventAction(),
  fEnergyAbs(0.),
  fEnergyGap(0.),
  fTrackLAbs(0.),
  fTrackLGap(0.),
  fEnergyACOL(0.),
  fEnergyPIPS(0.),
  fEnergyAPIPS(0.),
  fEnergyMYLAR(0.)
{}

//....ooo00000ooo.....ooo00000ooo.....ooo00000ooo.....ooo00000ooo.
.....

B4aEventAction::~B4aEventAction()
{}

//....ooo00000ooo.....ooo00000ooo.....ooo00000ooo.....ooo00000ooo.
.....

void B4aEventAction::BeginOfEventAction(const G4Event* /*event*/)
{
  // initialisation per event
  fEnergyAbs = 0.;
  fEnergyGap = 0.;
  fTrackLAbs = 0.;
  fTrackLGap = 0.;

  fEnergyACOL = 0.;
  fEnergyPIPS = 0.;
  fEnergyAPIPS = 0.;
  fEnergyMYLAR = 0.;
  fEnergyAll = 0.;
}

//....ooo00000ooo.....ooo00000ooo.....ooo00000ooo.....ooo00000ooo.
.....

void B4aEventAction::EndOfEventAction(const G4Event* event)
{
  // Accumulate statistics
  //

  // get analysis manager
  auto analysisManager = G4AnalysisManager::Instance();

  // fill histograms
  if(fEnergyACOL>0)  analysisManager->FillH1(0, fEnergyACOL);
  if(fEnergyAPIPS>0) analysisManager->FillH1(1, fEnergyAPIPS);
  if(fEnergyPIPS>0)  analysisManager->FillH1(2, fEnergyPIPS);
  if(fEnergyMYLAR>0) analysisManager->FillH1(3, fEnergyMYLAR);
  if(fEnergyAll>0)   analysisManager->FillH1(4, fEnergyAll);

  // fill ntuple
  // analysisManager->FillNtupleDColumn(0, fEnergyAbs);
  // analysisManager->FillNtupleDColumn(1, fEnergyGap);
  // analysisManager->FillNtupleDColumn(2, fTrackLAbs);
  // analysisManager->FillNtupleDColumn(3, fTrackLGap);
  //analysisManager->AddNtupleRow();

```

```

/* // Print per event (modulo n)
//
auto eventID = event->GetEventID();
auto printModulo = G4RunManager::GetRunManager()->GetPrintProgress();
if ( ( printModulo > 0 ) && ( eventID % printModulo == 0 ) ) {
    G4cout << "---> End of event: " << eventID << G4endl;

    G4cout
        << "    Absorber: total energy: " << std::setw(7)
            << G4BestUnit(fEnergyAbs,"Energy")
        << "        total track length: " << std::setw(7)
            << G4BestUnit(fTrackLAbs,"Length")
        << G4endl
        << "        Gap: total energy: " << std::setw(7)
            << G4BestUnit(fEnergyGap,"Energy")
        << "        total track length: " << std::setw(7)
            << G4BestUnit(fTrackLGap,"Length")
        << G4endl;
    }
}

/*
}

//.....ooo00000ooo.....ooo00000ooo.....ooo00000ooo.....ooo00000ooo.
.....

```

Stepping Action

```

/// \file B4aSteppingAction.cc
/// \brief Implementation of the B4aSteppingAction class

#include "B4aSteppingAction.hh"
#include "B4aEventAction.hh"
#include "B4DetectorConstruction.hh"

#include "G4Step.hh"
#include "G4RunManager.hh"

//.....ooo00000ooo.....ooo00000ooo.....ooo00000ooo.....ooo00000ooo.
.....

B4aSteppingAction::B4aSteppingAction(
    const B4DetectorConstruction* detectorConstruction,
    B4aEventAction* eventAction)
: G4UserSteppingAction(),
  fDetConstruction(detectorConstruction),
  fEventAction(eventAction)
{}

//.....ooo00000ooo.....ooo00000ooo.....ooo00000ooo.....ooo00000ooo.
.....

B4aSteppingAction::~B4aSteppingAction()
{}

//.....ooo00000ooo.....ooo00000ooo.....ooo00000ooo.....ooo00000ooo.
.....

void B4aSteppingAction::UserSteppingAction(const G4Step* step)
{

```



```

// Collect energy and track length step by step

// get volume of the current step
auto volume = step->GetPreStepPoint()->GetTouchableHandle()->GetVolume();

// energy deposit
auto edep = step->GetTotalEnergyDeposit();

///// step length
G4double stepLength = 0.;
if ( step->GetTrack()->GetDefinition()->GetPDGCharge() != 0. ) {
    stepLength = step->GetStepLength();
}

//std::cout<<"length    "<<stepLength<<std::endl;
//std::cout<<"Energy    "<<edep<<std::endl;
//std::cout<<"Volume    "<<volume<<std::endl;

if ( volume == fDetConstruction->GetACOLPV() ) {
    fEventAction->AddACOL(edep,stepLength);
}

if ( volume == fDetConstruction->GetPIPSPV() ) {
    fEventAction->AddPIPS(edep,stepLength);
}

if ( volume == fDetConstruction->GetAPIPSPV() ) {
    fEventAction->AddAPIPS(edep,stepLength);
}

if ( volume == fDetConstruction->GetMYLARPV() ) {
    fEventAction->AddMYLAR(edep,stepLength);
}

fEventAction->AddAll(edep, stepLength);

}

//....ooo00000ooo.....ooo00000ooo.....ooo00000ooo.....ooo00000ooo.

```

Run Action

```

/// \file B4RunAction.cc
/// \brief Implementation of the B4RunAction class

#include "B4RunAction.hh"
#include "B4Analysis.hh"

#include "G4Run.hh"
#include "G4RunManager.hh"
#include "G4UnitsTable.hh"
#include "G4SystemOfUnits.hh"

//....ooo00000ooo.....ooo00000ooo.....ooo00000ooo.....ooo00000ooo.
.....

B4RunAction::B4RunAction()
: G4UserRunAction()
{

```

```

// set printing event number per each event
G4RunManager::GetRunManager()->SetPrintProgress(1);

// Create analysis manager
// The choice of analysis technology is done via selectin of a namespace
// in B4Analysis.hh
auto analysisManager = G4AnalysisManager::Instance();
G4cout << "Using " << analysisManager->GetType() << G4endl;

// Create directories
//analysisManager->SetHistoDirectoryName("histograms");
//analysisManager->SetNtupleDirectoryName("ntuple");
analysisManager->SetVerboseLevel(1);
analysisManager->SetNtupleMerging(true);
    // Note: merging ntuples is available only with Root output

// Book histograms, ntuple
//

// Creating histograms
analysisManager->CreateH1("EACOL", "Edep in ACOL", 1000, 0., 10*MeV);
analysisManager->CreateH1("EAPIPS", "Edep in APIPS", 1000, 0., 10*MeV);
analysisManager->CreateH1("EPIPS", "Edep in PIPS", 1000, 0., 10*MeV);
analysisManager->CreateH1("EMYLAR", "Edep in MYLAR", 1000, 0, 10*MeV);
analysisManager->CreateH1("EAll", "Edep all", 1000, 0., 10*MeV);

//analysisManager->CreateH1("Labs", "trackL in absorber", 100, 0., 1*m);
//analysisManager->CreateH1("Lgap", "trackL in gap", 100, 0., 50*cm);

// Creating ntuple
//
//analysisManager->CreateNtuple("B4", "Edep and TrackL");
//analysisManager->CreateNtupleDColumn("Eabs");
//analysisManager->CreateNtupleDColumn("Egap");
//analysisManager->CreateNtupleDColumn("Labs");
//analysisManager->CreateNtupleDColumn("Lgap");
//analysisManager->FinishNtuple();
}

//....ooo00000ooo.....ooo00000ooo.....ooo00000ooo.....ooo00000ooo.
.....

B4RunAction::~B4RunAction()
{
    delete G4AnalysisManager::Instance();
}

//....ooo00000ooo.....ooo00000ooo.....ooo00000ooo.....ooo00000ooo.
.....

void B4RunAction::BeginOfRunAction(const G4Run* /*run*/)
{
    //inform the runManager to save random number seed
    //G4RunManager::GetRunManager()->SetRandomNumberStore(true);

    // Get analysis manager
    auto analysisManager = G4AnalysisManager::Instance();

    // Open an output file
    //
    G4String fileName = "B4";

```

```

    analysisManager->OpenFile(fileName);
}

//.....ooo00000ooo.....ooo00000ooo.....ooo00000ooo.....ooo00000ooo.
.....

void B4RunAction::EndOfRunAction(const G4Run* /*run*/)
{
    // print histogram statistics
    //
    auto analysisManager = G4AnalysisManager::Instance();
    if ( analysisManager->GetH1(1) ) {
        G4cout << G4endl << " ----> print histograms statistic ";
        if(isMaster) {
            G4cout << "for the entire run " << G4endl << G4endl;
        }
        else {
            G4cout << "for the local thread " << G4endl << G4endl;
        }

        G4cout << " EAbs : mean = "
            << G4BestUnit(analysisManager->GetH1(0)->mean(), "Energy")
            << " rms = "
            << G4BestUnit(analysisManager->GetH1(0)->rms(), "Energy") <<
G4endl;

        G4cout << " EGap : mean = "
            << G4BestUnit(analysisManager->GetH1(1)->mean(), "Energy")
            << " rms = "
            << G4BestUnit(analysisManager->GetH1(1)->rms(), "Energy") <<
G4endl;

        G4cout << " LAbs : mean = "
            << G4BestUnit(analysisManager->GetH1(2)->mean(), "Length")
            << " rms = "
            << G4BestUnit(analysisManager->GetH1(2)->rms(), "Length") << G4endl;

        G4cout << " LGap : mean = "
            << G4BestUnit(analysisManager->GetH1(3)->mean(), "Length")
            << " rms = "
            << G4BestUnit(analysisManager->GetH1(3)->rms(), "Length") << G4endl;
    }

    // save histograms & ntuple
    //
    analysisManager->Write();
    analysisManager->CloseFile();
}

//.....ooo00000ooo.....ooo00000ooo.....ooo00000ooo.....ooo00000ooo.
.....

```

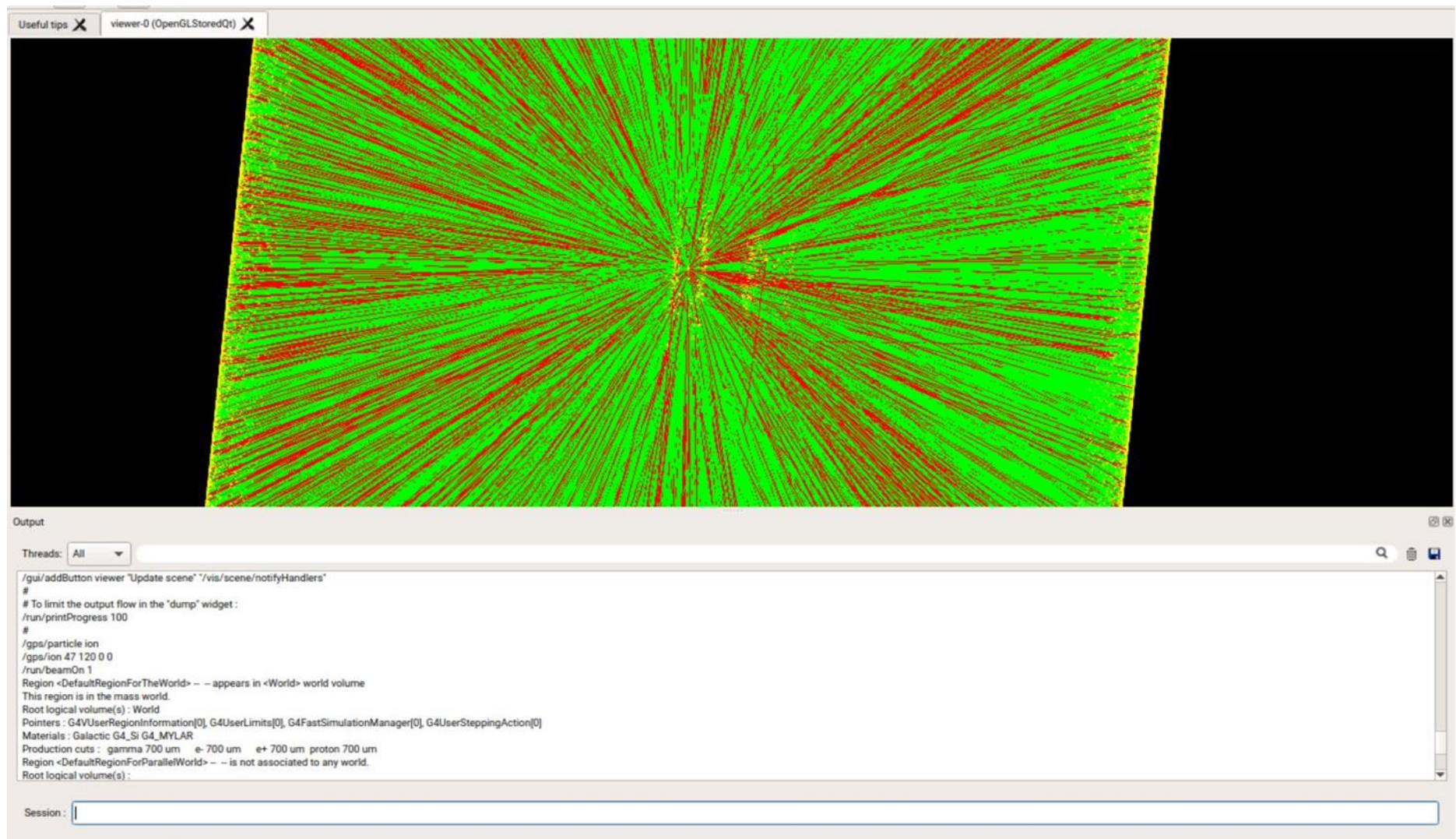


Figure 7.1: $1\text{E}10^7$ beta decay in the DSS+

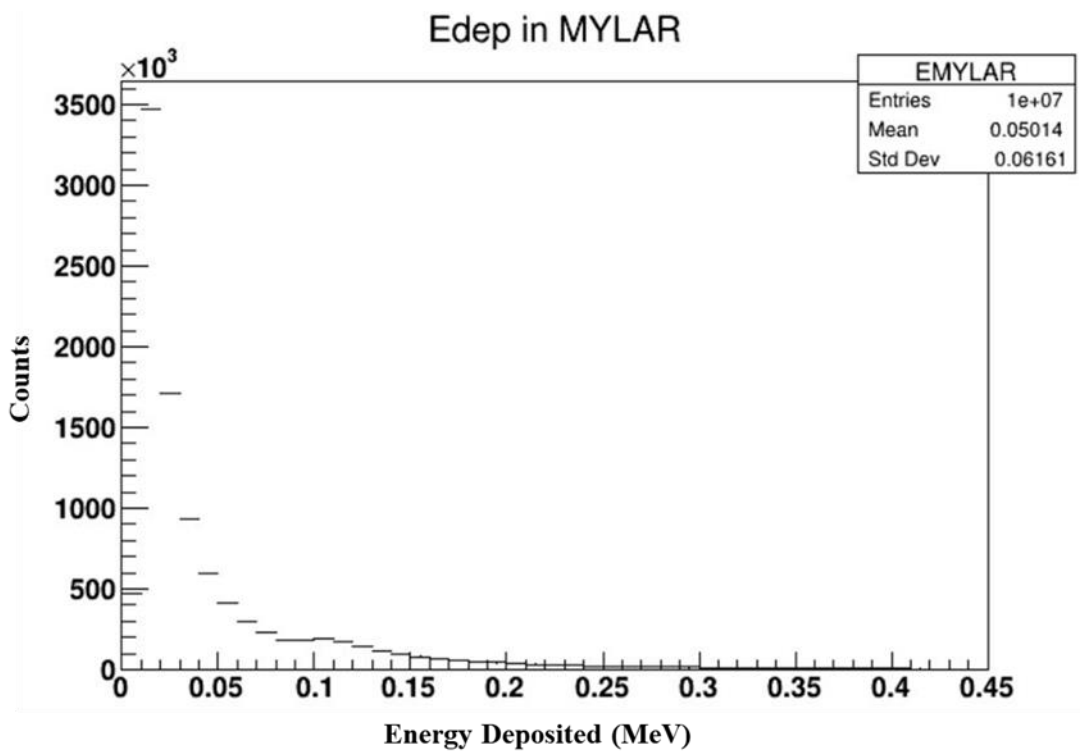


Figure 7.2: Simulation for 1×10^7 beta events on Mylar® Tape

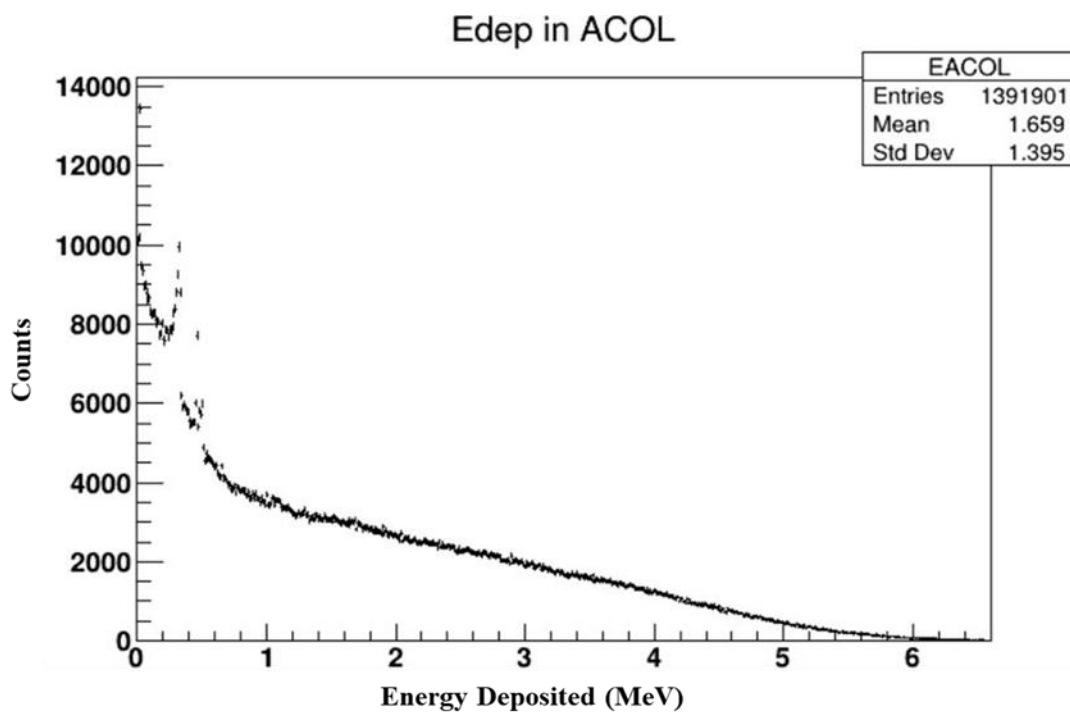


Figure 7.3: Simulation for 1×10^7 beta events on ACOL

